Supplemental Data

Infectious Neutrophil deployment is regulated by Resolvin D4

Stephania Libreros, Robert Nshimiyimana, Brendon Lee, and Charles N. Serhan

Center for Experimental Therapeutics and Reperfusion Injury,
Department of Anesthesiology, Perioperative and Pain Medicine, Brigham and Women's Hospital and Harvard Medical School, Boston, Massachusetts 02115, USA.

Keywords: lipid mediator, myelopoiesis, specialized pro-resolving mediators, resolution lipidomics, essential fatty acids

Address correspondence and reprint requests to:
Prof. Charles N. Serhan, Director
Center for Experimental Therapeutics and Reperfusion Injury,
60 Fenwood Rd., Hale Building for Transformative Medicine 3-016, Boston, Massachusetts 02115, USA.
Phone: 617-525-5001; Fax: 617-525-5017
E-mail: cserhan@bwh.harvard.edu

This PDF includes:

Suplemental Methods
Figure S1-S6
Tables S1-S7

Supplemental Methods

Murine Peritonitis

Male FVB mice (6- to 8-weeks-old, purchased from Charles River, MA) were fed ad lib a Rodent Diet 20 containing 0.02% arachidonic acid and 0.42% omega-3 fatty acids: 20 times more omega-3 than omega-6 fatty acids. Mice were inoculated i.p. with live *E. coli* (serotype O6:K2:H1 at 10^5 CFU/mouse) in sterile saline as reviewed in[1] and recently in[2]. At the designated time intervals, mice were euthanized with isoflurane and infectious exudates (peritoneal lavage), whole blood, and BM cells were collected for flow cytometry, single-cell mass cytometry analysis and SPM-targeted metabololipidomics profiling (vide infra). Leukocyte populations from each mouse organ were determined by flow cytometry. For bacterial titers, aliquots of each exudate were plated onto LB agar plates and incubated overnight at 37ºC. The next day, LB plates were photographed and enumerated using ImageJ software (Version 1.53, NIH).

Mass Cytometry (CyTOF)

Mouse Cells: Exudates (peritoneal lavage), whole blood and bone marrow cells were obtained as described above. Immediately after collection, cells were fixed with 1.6% paraformaldehyde for 10 minutes at room temperature. A portion of the cells was then barcoded with palladium isotopes according to the manufacturer's protocol (Pd 102, 104, 105, 108, and 110). All CyTOF reagents were purchased from Fluidigm (San Francisco, CA) as in [3]. Cells were then washed twice using the barcode permeabilization buffer. The diluted barcodes were transferred to the cells and incubated for 30 minutes at room temperature. The barcoded cells were washed twice in CyTOF staining buffer ($DPBS^{++}$ with 0.5% BSA and 0.1% sodium azide) and then pooled for staining. Pooled barcoded cells were incubated for 10 minutes at room temperature with FcX block (Biolegend) for Fc receptor–mediated nonspecific antibody binding. Barcoded cells were stained for 30 minutes with metal label surface antibodies at room temperature, then washed twice in CyTOF staining buffer. All surface antibodies are listed in **Table S4** [4]. Cells were then washed twice and stained in 1ml of 1:1,000 Cell-ID Iridium intercalator (diluted in DPBS) for 12 hours at 4°C. Next, cells were washed twice in CyTOF staining buffer, twice with Maxpar Cell Acquisition solution, and then reconstituted with Cell Acquisition Solution (CAS) at a concentration of $5x10^6$ cells/mL containing EQ calibration beads (EQ four elements Calibration Beads, Fluidigm, San Francisco, CA). Cells were filtered through a 35-μm nylon mesh filter cap

(Corning, Falcon). Barcoded cells were analyzed on Helios CyTOF (Fluidigm, San Francisco, CA) at an event rate of 400 to 500 cells per second. Data (FCS files) were normalized using Helios Software v6.3.119 at the Longwood Medical Area LMA CyTOF facility at Dana Farber Cancer Institute (Boston, MA, USA). The files were debarcoded using the Fluidigm Debarcoder application, gating was performed in the FlowJo v10 software (BD), and FCS files were exported for analysis.

Human bone marrow cells: Human BM cells ($2x10^6$cells/0.5 mL $DPBS^{+/+}$) were incubated with RvD4 [10^{-8}M] or vehicle alone (0.01% ethanol *vol/vol*) for 0, 5, or 15 min at 37ºC, pH 7.45. Samples were barcoded as described above and stained with a panel of 28 metal-conjugated human surface antibodies, as listed in **Table S5**[5]. Cells were permeabilized in 80% cold methanol (-20°C) and stained with seven metal-conjugated antibodies for intracellular phosphorylated signaling proteins as listed in **Table S5.** Samples were normalized and debarcoded as described above.

CyTOF Data Analysis

Mouse ($CD45^+CD41^-$) and human bone marrow single cells were analyzed using R environment (version 4.0.5 and 4.1.0) (http://www.r-project.org/) and Bioconductor packages (https://www.bioconductor.org). FCS files were imported into R using flowCore (2.4.0), and the data was normalized and clustered using the CATALYST package (1.16.0)[6]. Specifically, surface marker expression and phosphorylation levels were normalized using an inverse hyperbolic sine transformation (arsinh) with a cofactor of 5. Clustering was performed using FlowSOM[7] (2.0.0)—which builds a self-organizing map (SOM), connects the nodes of the SOM through a minimal spanning tree, and clusters the SOM nodes—to identify immune cell metaclusters. Metaclusters were then merged according to surface marker expression.

Dimensionality reduction was performed using the CATALYST package[6]. Uniform manifold approximation and projection (UMAP) plots were used to visualize the clustering of individual cells and their expression of surface markers in 2-dimensional space. UMAP is particularly effective at visualizing larger datasets since it conserves both the local and global structure of the data, which facilitates understanding of how immune cell populations differ between treatments, timepoints, and organs[8].

Differential abundance and marker expression analyses were performed using the diffcyt package[9] (1.12.0), which enables the convenient use of various statistical frameworks. For differential abundance analysis, edgeR (3.34.0) was used; this algorithm utilizes a negative binomial distribution to model the abundance of the immune cell populations and to determine statistical significance. For differential marker expression, we used limma (3.48.0), which fits a linear model to each marker expression and calculates empirical Bayes moderated t-statistics tests at the cluster level.

The VorteX clustering environment was downloaded from https://github.com/nolanlab/vortex. Manually gated $CD45^+CD41^-$ were uploaded into the VorteX clustering environment following algorithm settings as in [10]. Briefly, the following settings were used: 1) Numerical transformation: arcsinh cofactor 5, 2) noise threshold: 1.0, 3) feature rescaling: none, 4) normalization: none, 5) distance measure: angular distance, 6) Clustering algorithm: X-shift (gradient assignment), 7) Density estimate: N nearest neighbors, 8) the number of neighbors for density estimate (K): from 150 to 5, with 15 steps, and 9) number of neighbors for mode finding (N): determine automatically. These clustering settings were as recommended in [10]. Following clustering, the K-values of the elbow-shape plot (as in Fig. 2D-E), between the linear and exponential phase, were calculated. A force-directed layout was created and clusters annotated as described in [10]. The clusters were colored according to each immune phenotype.

Pseudotime-based trajectory analyses (as in Fig. 6D-F) were performed using Slingshot[11] (1.8.0). Slingshot identifies cell lineages and arranges them in pseudotime by constructing a cluster-based minimum spanning tree to identify key elements of the lineage structure and then fits smooth curves along these elements[11]. When calculating trajectories, LSKs ($Lineage^-SCA1^+CD117^+CD150^+CD48^+$) were specified as the start cluster and Diffusion maps was the dimensionality reduction and used to perform the calculations.

Targeted lipid mediator (LM) metabolipidomics

Murine bone marrow samples were collected and 500 pg of each deuterated internal standard, *d*8-5-HETE, *d*8-12-HETE, *d*8-15-HETE, *d*4-LTB_4, *d*5-LXA_4, *d*5-RvD2, *d*5-RvD3, and *d*4-PGE_2 (Cayman Chemical Company, Ann Arbor, MI) were added in two volumes of ice-cold methanol (Thermo Fisher Scientific, Waltham, MA). The addition of deuterium-labeled internal standards was used to quantify sample recoveries. The chromatographic regions

containing monohydroxy, dihydroxy and trihydroxy mediators were calculated based on the corresponding deuterium-labeled standard, since deuterium labels are not yet available for all the lipid mediators. Bone marrow samples were kept at -80^{o}C prior to extraction and LC-MS/MS metabololipidomics analysis. Samples were thawed on ice followed by centrifugation (3000 rpm, 10 min, 4^{o}C). Methanolic supernatants were collected from each sample and concentrated to ~1 mL using a gentle stream of nitrogen gas (Turbo Vap LV, Biotage, Charlotte, NC).

Solid-phase extractions were carried out using the automated platform Extrahera^{TM} (Biotage, Charlotte, NC) as in[3]. Bone marrow samples were applied to C18 ISOLUTE 100-mg SPE cartridges (Biotage, Charlotte, NC), which were equilibrated with 3 mL of methanol and 3 mL of double-distilled water. Next, samples were acidified with 9 mL of water (pH 3.5, HCl), rapidly loaded into the conditioned C18 columns, and washed with 4 mL of double-distilled water. Then, 4 mL of hexane (Supelco, Bellefonte, PA) were added to elute non-polar molecular species. Next, lipid mediator (LM) products of interest were eluted in 4 mL of methyl formate (Sigma-Aldrich, St. Louis, MO) and taken to dryness under a gentle stream of nitrogen (Turbo Vap LV, Biotage, Charlotte, NC). Samples were then immediately resuspended in 50 µL of methanol/ water, 1:1, *v*/*v* mixture, and metabololipodomics analysis was carried out in negative ion mode on triple quadrupole LC-MS/MS systems.

Bone marrow samples were run on a triple quadrupole QTRAP 5500 mass spectrometer (SCIEX, Framingham, MA) equipped with a Shimadzu LC-20AD HPLC and a Shimadzu SIL-20AC autoinjector (Shimadzu, Kyoto, Japan). The column implemented in this system was a Poroshell 120 EC-18 column (100 mm x 4.6 mm x 2.7 µm; Agilent Technologies, Santa Clara, CA), housed in a column oven maintained at 50^{o}C, and LMs were eluted in a gradient of methanol water/acetic acid from 55:45:0.01 (*v*/*v*/*v*) to 98:2:0.01 at a 0.5 mL/min flow rate. Targeted multiple reaction monitoring (MRM) and enhanced product ion (EPI) scanning in negative ion mode were used to monitor and quantify the mediators (**Table S6**). RvD1 and RvD4 physical properties were validated using a QTRAP 6500+ LC-MS/MS system (SCIEX, Framingham, MA) equipped with a SCIEX ExionLC (SCIEX, Framingham, MA) in negative polarity and low-mass mode on a Kinetex Polar C18 column (100 mm x 4.6 mm x 2.6 µm; Phenomenex, Torrance, CA, USA) maintained at 50°C (**Table S6**).

Data acquisition parameters were individually optimized for each targeted mediator based on their unique chromatographic and spectral properties. **Table S7** lists polarity, Q1 (*m/z*), Q3

(*m/z*), declustering potential (DP, V), entrance potential (EP, V), collision energy (CE, V), and collision cell exit potential (CXP, V) for each identified LM.

Each lipid mediator was identified by matching their chromatographic retention times and ions present in the MS/MS spectra using an unbiased library search with those of known stereochemistry. A customized lipid mediator library was constructed using both synthetic materials prepared from total organic synthesis (Cayman Chemical, MI) and authentic SPMs prepared from human leukocytes.

Each MS/MS spectra from endogenous SPMs was matched to the corresponding synthetic standard. Criteria for a positive match were set at ≥70% match (fit) score with our library. The library matching parameters were set as follows: precursor mass tolerance ± 0.8 Da; collision energy ± 5 eV; use polarity, intensity threshold = 0.05; minimal purity = 5.0%; and intensity factor = 100. The MS/MS spectral library uses searching algorithms to calculate a fit score, which is determined using the ions that occur in the library MS-MS spectrum. This score shows the degree to which the library spectrum is contained in the sample (or unknown) spectrum. Data were acquired with Analyst 1.7.1 software (SCIEX), and the MS/MS spectral library was constructed in LibraryView^{TM} software version 1.4.0 (SCIEX) in conjunction with SCIEX OS software version 1.7.0.36606 (SCIEX). LC-MS/MS MRM traces and MS/MS spectra are presented as direct screen captures from SCIEX OS (SCIEX).

Myeloid and Hematopoietic Stem-Progenitor Cell (HSPC) Flow Cytometry

Mouse peritoneal *E. coli* exudates, whole blood, and bone marrow cells were suspended in fluorescence-activated cell sorting (FACS) buffer (DPBS with 1% bovine serum albumin (BSA) and 0.1% sodium azide) and incubated with FC receptor block (15 min, 4°C; BD PharMingen) or rat serum. Cell viability was then assessed using Fixable Aqua Dead stain (ThermoFisher).

Next, these peritoneal exudates, whole blood, and bone marrow cells were incubated with anti-mouse PerCP/Cy5.5 CD45, anti-mouse PE/Cy7 CD11b, anti-mouse APC F4/80, anti-mouse FITC Ly6C, anti-mouse PE Ly6G, and appropriate isotype control for the identification of neutrophils ($CD45^{+}CD11B^{+}Ly6G^{+}Ly6C^{-}F4/80^{-}$), monocytes ($CD45^{+}CD11B^{+}Ly6C^{+}Ly6G^{-}F4/80^{-}$) and macrophages ($CD45^{+}CD11B^{+}Ly6G^{-}Ly6C^{-}F4/80^{+}$).

***In vivo* exudate *E. coli* phagocytosis.** Mouse peritoneal leukocytes were collected at 12hrs after peritonitis. Peritoneal exudates were stained with surface antibodies anti-mouse

PerCP/Cy5.5 CD45, anti-mouse APC F4/80, anti-mouse PE-Cy7 Ly6G, and anti-mouse APC-Cy7 Ly6G for the identification of neutrophils, monocytes, and macrophages. Exudates were then permeabilized using the BD cytoperm™ permeabilization buffer (BD Biosciences, CA) for 45 min following the manufacturer's protocol. Exudates were washed twice with BD Perm/Wash buffer (BD Biosciences, CA). Fc receptor- mediated, non-specific antibody binding was blocked by TruStain FcX anti-mouse CD16/CD32 antibody and sequentially stained for intracellular *E. coli* using a FITC-conjugated anti-*E. coli* antibody (1: 50 dilution) (GTX40856; Genetics). Cells were then taken to flow cytometry to assess % intracellular *E. coli* (FITC+) in macrophages ($CD45^+Ly6G^-Ly6C^-F4/80^+$), neutrophils ($CD45^+F4/80^-Ly6C^-$ $Ly6G^+$) and monocytes ($CD45^+Ly6G^-F4/80^-Ly6C^+$).

***In vivo* macrophage efferocytosis of apoptotic neutrophils**. Peritoneal exudates were collected at 12hrs. Cells were stained with TruStain FcX anti-mouse CD16/CD32 antibody following staining with anti-mouse PerCP/Cy5.5 CD45, APC F4/80, and anti-mouse PE-Cy7 CD11b. Exudates were then permeabilized using the BD cytopermTM permeabilization buffer (BD Biosciences, CA) for 45 minutes following the manufacturer's protocol. Cells were washed twice with BD Perm/Wash buffer (BD Biosciences, CA) and resuspended in FACS buffer (DPBS, 5% FBS, 2nM EDTA, 2nM NaN3). Fc receptor- mediated, non-specific antibody binding was blocked by TruStain FcX anti-mouse CD16/CD32 antibody, which was followed by incubation with PE anti-mouse Ly6G (1:100) (Biolegend, CA) or PE Isotype control. Cells were analyzed by flow cytometry to determine the % of macrophages ($CD45^+CD11b^+F4/80^+$) and efferocytosis of neutrophils ($Ly6G^+$).

***In vivo* neutrophil viability**. Peritoneal exudates were collected at 12hrs. Exudates were stained with TruStain FcX anti-mouse CD16/CD32 antibody following incubation with anti-mouse PerCP/Cy5.5 CD45 and anti-mouse APC-Cy7 Ly6G for 30 mins for the identification of neutrophils. Cells were then washed and stained with FITC-conjugated Annexin V (BD Biosciences, CA) and propidium iodide (PI) according to the manufacturer's protocol. Live cells were immediately analyzed using BD LSRFortessa (BD Biosciences, CA).

Identification of Bone Marrow HSPCs. Femurs, and tibias from mice with *E. coli* peritonitis were flushed with 2 mL of IMDM Medium (25mM HEPES and 2% FBS) following red blood cell lysis (Biolegend, CA). Cells were then stained with FITC-labeled anti-mouse lineage cocktail (anti-mouse CD3, anti-mouse CD45R, anti-mouse CD11b, anti-mouse TER-119) (Thermo

Fisher Scientific), anti-mouse Ly6G, PE-anti mouse SCA-1, APC anti-mouse cKit, APC-Cy7 anti-mouse CD16/32, PerCP-Cy5.5 anti-mouse CD34, and appropriate isotype control for the identification of BM-LSK (Lin^- $Sca\text{-}1^+$ $cKit^+$), granulocyte monocyte progenitor (GMP) and common myeloid progenitor (CMP) [12].

Murine Bone Marrow Intracellular Signaling Bone marrow cells were isolated from *Fpr2* KO (*Alx/Fpr2*$^{-/-}$, ALX deficient mice) or *Fpr2* floxed (*hALX/FPR*$^{fl/fl}$) mice[13]. BM single-cell suspensions were incubated with 10nM of either RvD1 or RvD4 or vehicle alone (0.01% ethanol vol/vol) for 0, 1, 5, and 15 minutes and at 37°C. Cells were fixed and permeabilized using 80% ice-cold methanol for 10 minutes at –20°C and washed twice. Cells were first stained with PerCP/Cy5.5 CD45, anti-mouse PE-Cy7 Ly6G, and anti-mouse APC-Cy7 Ly6G for the identification of BM neutrophils and monocytes. Next, cells we're incubated with TruStain FcX anti-mouse CD16/CD32 antibody for 10 mins and stained with PE-pERK1/2 (T202/Y204) (clone MILAN8R) (ebioscience, San Diego) or PE-STAT3 (Tyr705) (clone 13-A-3-1) and respective Isotype controls. Levels of pERK1/2 and pSTAT3 were then assessed using flow cytometry.

Human Neutrophil Intracellular calcium release

Human peripheral whole blood samples were labeled with Indo-1 AM dye (eBioscience) at 37°C for 30 minutes. Samples were analyzed using BD FACSymphony (BD Biosciences) at approximately 2,000–2,500 events/seconds for 5 minutes to establish the Ca^{2+} baseline with an Indo-1 AM signal, then 10 nM of LTB_4, RvD1, RvD4 were added to samples and recorded for another 10 minutes. All samples were analyzed using FlowJo.

Human Neutrophil Whole Blood Phagocytosis

Human peripheral whole blood (300 μL) was incubated with either RvD4 (0.1 nM, 1 nM, 10 nM, or 100nM) or vehicle alone (containing 0.01% ethanol *vol/vol*) for 15 minutes at 37ºC before the addition of labeled *E. coli*. Bacteria was labeled using Baclight Green fluorescent dye according to the manufacturer's protocol (Life Technologies, Grand Island, NY). Labeled *E. coli* (1:50, leukocytes to *E. coli*) was added to samples to initiate phagocytosis at 37◦C for 45 min. Samples were then incubated with PE anti-human CD15 (neutrophils) and APC-Cy7 anti-human CD14 (monocytes) (Biolegend, San Diego, CA) for 15 min on ice. Cells were washed twice with 2mL of ice-cold PBS followed by red blood cell lysis and fixed in 2% paraformaldehyde. Cells were then analyzed using BD LSRFortessa (BD Biosciences, CA). Fluorescent associated phagocytosis was measured in $CD15^+CD14^-$ in human neutrophils.

All flow cytometric samples were assessed using FACSDiva Canto II or BD LSRFortessa (BD Biosciences, Franklin Lakes, NJ) and analyzed using FlowJo software v10 (BD) as in [12]. Debris [forward scatter (FSC)-area (A) *vs.* side scatter (SSC)-A] and doublets (FSC-height (H) *vs.* FSC-A → FSC-A *vs.* FSC-width (W) → SSC-H *vs.* SSC-A) were excluded before further gating on populations.

Neutrophil Mobilization: Naïve FVB male mice were administered i.v. either LTB_4 (100ng/mouse), RvD4 (100 ng/mouse), vehicle (0.01% ethanol in saline *vol/vol*) or pretreatment with RvD4 followed by LTB_4. In the combined (RvD4, LTB_4) set of mice, RvD4 (100ng/mouse) was administered i.v. 10 minutes prior to LTB_4 (100ng/mouse) injection. At indicated time intervals (0, 5, 10, 15, 20, 30, 40 and 60 min), whole blood samples were collected. Whole blood neutrophils were enumerated and differentially counted using Turk's solution and light microscopy.

Hematopoietic Colony-Forming Units (CFU)

Bone marrow cells were obtained from 8-week-old FVB naïve mice. Bones were flushed in IMDM Medium (25mM HEPES and 2% FBS) and incubated in red blood cell lysis buffer (Biolegend, CA, USA). Bone marrow cells were seeded (10^4 per plate per condition) in duplicates in 35mm STEMgridTM-6 Counting Grid plates (Stem Cell Technologies, Vancouver, BC) and cultured in mouse methylcellulose media containing 15% FBS, 2% BSA, rh-insulin 10ug/mL, rtransferrin 200ug/mL, rm-SCF 50ng/mL, rm-IL-13 10ng/mL, and rmIL-6 10ng/mL (R&D system, Minneapolis, MN) at 37ºC, pH 7.5, as described in the manufacturer's protocol. Plated cells were then treated in the presence of RvD1 (0.01nM, 0.1nM, 1nM and 10nM) and RvD4 (0.01nM, 0.1nM, 1nM and 10nM) or vehicle (0.01% ethanol *vol/vol*) at time 0 and 72 hours.

In a separate set of experiments, bone marrow cells were obtained at 12hrs from mice with self-limited peritonitis infections (Vehicle or RvD4 groups). Bones were flushed as described above. Bone marrow cells were seeded (10^4 per plate per condition) in triplicates in 35mm gridded Nunc Cell Culture Dishes (ThermoFisher Scientific, MA), and cultured in mouse methylcellulose media containing 15% FBS, 2% BSA, rh-insulin 10μg/mL, rtransferrin 200μg/mL, rm-SCF

50ng/mL, rm-IL-13 10ng/mL, and rmIL-6 10ng/mL (R&D Systems, Minneapolis, MN) at 37ºC, pH 7.5.

Subsequently, colonies developed from individual cells on Day 12 were morphologically evaluated and enumerated in terms of colony-forming units (CFU) for CFU-G: granulocytes, CFU-M: myocytes and CFU-GM: granulocyte/macrophage using inverted light microscopy.

Real-time imaging single-cell phagocytosis

Naïve peritoneal macrophages (MΦ) were plated onto 8-well chamber slides (1×10^5 cells/well in $DPBS^{++}$). MΦ were incubated with RvD4 (10^{-10} M to 10^{-8} M) or vehicle alone (0.01% ethanol *vol/vol*) for 15 minutes prior to the initiation of phagocytosis with BacLight Green-labeled *E. coli* (5×10^6 CFUs). The chamber slides were kept in a stage-top incubator system for microscopes equipped with a built-in digital gas mixer and temperature regulator (TOKAI HIT model INUF-K14). Images were then acquired every 10 minutes for 120 minutes (37°C) with a Keyence BZ-9000 (BIOREVO) inverted fluorescence phase-contrast microscope (20X objective) equipped with a monochrome/color-switching camera using BZ-II Viewer software as in[3]. Green fluorescence intensity was quantified using the BZ-II Analyzer software.

Murine Bone Marrow Macrophage Efferocytosis

Isolation of Bone Marrow Neutrophils**:** BM cells were harvested from FVB naïve mice by flushing with IMDM Medium (25mM HEPES and 2% FBS). Neutrophils were isolated using EasySep™ mouse neutrophil enrichment kit (Stem Cell Technologies, Canada). The purity of Ly6G positive neutrophils was greater than 96% using this method assessed by flow cytometry. BM neutrophils were cultured for 12hrs in complete media (RPMI supplemented with 10% fetal bovine serum plus penicillin/streptomycin), then washed with 2mM EDTA and counted for efferocytosis. Then, BM neutrophils were labeled with PKH67 Green Fluorescent Cell linker labeling kit following the manufacturer's protocol (Sigma-Aldrich) and used for Bone Marrow-Derived Macrophage (BMDM) efferocytosis studies using confocal microscopy.

Bone Marrow-Derived Macrophage (BMDM) Isolation, Culture, and Efferocytosis: Femurs and tibias from naïve FVB mice were flushed in 2 mL of IMDM Medium (25mM HEPES and 2% FBS) following red blood cell lysis (Biolegend, CA). BMDMs culture in medium containing basal

medium supplemented with 20% L929 conditioned medium for seven days. On day 7 of differentiation, cells were liberated with a cell scraper, collected, and spun at 400 × *g* for 10 min. The cells were then resuspended in basal medium, enumerated, and seeded in a six-well Corning Costar flat-bottom cell culture plate (ThermoFisher Scientific, MA) at a cell density of 2 x 10^6 cells per well for 24 hours. BMDMs were washed twice with DPBS via aspiration (ThermoFisher Scientific, MA) to eliminate cellular debris. Cells were then incubated with either RvD4 (10^{-11} M to 10^{-7} M) or vehicle alone (0.01% ethanol *vol/vol*) for 15 minutes before the addition of CFSE-labelled apoptotic neutrophils [1:5 (BMDM: neutrophils) ratio]. After 120 minutes of co-incubation at 37°C, plates were washed thoroughly to remove non-ingested cells, and BMDMs were fixed with 2% paraformaldehyde for 15 minutes at 4°C. The cells were washed with DPBS and scraped. BMDMs were then permeabilized using the BD cytopermTM permeabilization buffer (BD Biosciences, CA) for 45 minutes following the manufacturer's protocol. Cells were washed twice with BD Perm/Wash buffer (BD Biosciences, CA), resuspended in FACS buffer (DPBS, 5% FBS, 2nM EDTA, 2nM NaN3), and stained with APC-Cy7 anti-mouse Ly6G (1:100) (Biolegend, CA). BMDMs were then taken to flow cytometry to assess efferocytosis ($CFSE^+Ly6G^+$) via dual labeling. All flow cytometric samples were assessed using BD LSRFortessa (BD Biosciences, CA), and percent efferocytosis (% $CFSE^+Ly6G^+$ macrophages) was quantified using FlowJo v10 software.

Confocal Microscopy: BMDMs (1×10^5 cells/well) were seeded on gelatin-coated glass coverslips in a 12-well plate for 24 h. BMDMs were treated with RvD4 (1nM) or vehicle alone (0.01% ethanol vol/vol) for 15 minutes prior to the addition of purified unlabeled or PKH67 green fluorescently labeled aged neutrophils (1:5 BMDM: neutrophil) for 120 minutes. Cells were then fixed with 2% paraformaldehyde (15 min), followed by incubation in 0.25% Triton X-100 (Sigma-Aldrich) containing Background Sniper (10 min, room temperature) to reduce background staining. Cells were then incubated with rhodamine-phalloidin (Life Technologies) for 30 min for actin visualization, followed by incubation with mouse monoclonal anti-Ly6G (clone EPR22909-135, Abcam) (1:200) overnight at 4°C for unlabeled apoptotic neutrophils. Coverslips were then washed and labeled with the following secondary antibodies: Alexa Fluor 647 donkey anti-rabbit (1:1000) or Cy5 (1:200) (Life Technologies) for unlabeled apoptotic BM-neutrophils. To visualize the nuclei, the coverslips were mounted with VECTASHIELD containing DAPI (Vector Laboratories). Efferocytosis static and Z stack images were visualized on a Zeiss LSM 800 with an Airyscan-Axio Observer Z1 inverted confocal system with a 20 or 63X objective and Zen version 3.3.89.0000 software in the Confocal Core at Brigham and Women's Hospital. For all

direct comparisons, samples were stained and imaged on the same day with the same settings. 3D efferocytosis movies were formatted using Zen 3.3 software (version 3.3.89.0000, blue edition).

Software

Chemical structures were drawn using ChemDraw Level Professional v20.1.0.112 and Chem3D v21.0.0 (PerkinElmer, Waltham, MA).

References

1. Serhan CN. Pro-resolving lipid mediators are leads for resolution physiology. *Nature*. 2014;510(7503):92-101.

2. Serhan CN, Libreros S, Nshimiyimana R. E-series resolvin metabolome, biosynthesis and critical role of stereochemistry of specialized pro-resolving mediators (SPMs) in inflammation-resolution: Preparing SPMs for long COVID-19, human clinical trials, and targeted precision nutrition. *Semin Immunol*. 2022:101597.

3. Norris PC, Libreros S, Chiang N, Serhan CN. A cluster of immunoresolvents links coagulation to innate host defense in human blood. *Sci Signal*. 2017;10(490).

4. Severe N, Karabacak NM, Gustafsson K, Baryawno N, Courties G, Kfoury Y, Kokkaliaris KD, Rhee C, Lee D, Scadden EW, Garcia-Robledo JE, Brouse T, Nahrendorf M, Toner M, Scadden DT. Stress-Induced Changes in Bone Marrow Stromal Cell Populations Revealed through Single-Cell Protein Expression Mapping. *Cell Stem Cell*. 2019.

5. Dinh HQ, Eggert T, Meyer MA, Zhu YP, Olingy CE, Llewellyn R, Wu R, Hedrick CC. Coexpression of CD71 and CD117 Identifies an Early Unipotent Neutrophil Progenitor Population in Human Bone Marrow. *Immunity*. 2020;53(2):319-334 e316.

6. Nowicka M, Krieg C, Crowell HL, Weber LM, Hartmann FJ, Guglietta S, Becher B, Levesque MP, Robinson MD. CyTOF workflow: differential discovery in high-throughput high-dimensional cytometry datasets. *F1000Res*. 2017;6:748.

7. Van Gassen S, Callebaut B, Van Helden MJ, Lambrecht BN, Demeester P, Dhaene T, Saeys Y. FlowSOM: Using self-organizing maps for visualization and interpretation of cytometry data. *Cytometry A*. 2015;87(7):636-645.

8. Becht E, McInnes L, Healy J, Dutertre CA, Kwok IWH, Ng LG, Ginhoux F, Newell EW. Dimensionality reduction for visualizing single-cell data using UMAP. *Nat Biotechnol*. 2018.

9. Weber LM, Nowicka M, Soneson C, Robinson MD. diffcyt: Differential discovery in high-dimensional cytometry via high-resolution clustering. *Commun Biol*. 2019;2:183.

10. Samusik N, Good Z, Spitzer MH, Davis KL, Nolan GP. Automated mapping of phenotype space with single-cell data. *Nat Methods*. 2016;13(6):493-496.

11. Street K, Risso D, Fletcher RB, Das D, Ngai J, Yosef N, Purdom E, Dudoit S. Slingshot: cell lineage and pseudotime inference for single-cell transcriptomics. *BMC Genomics*. 2018;19(1):477.

12. Galvin A, Weglarz M, Folz-Donahue K, Handley M, Baum M, Mazzola M, Litwa H, Scadden DT, Silberstein L. Cell Cycle Analysis of Hematopoietic Stem and Progenitor Cells by Multicolor Flow Cytometry. *Curr Protoc Cytom*. 2019;87(1):e50.

13. Sansbury BE, Li X, Wong B, Patsalos A, Giannakis N, Zhang MJ, Nagy L, Spite M. Myeloid ALX/FPR2 regulates vascularization following tissue injury. *Proceedings of the National Academy of Sciences*. 2020;117(25):14354-14364.

Supplemental Figure1

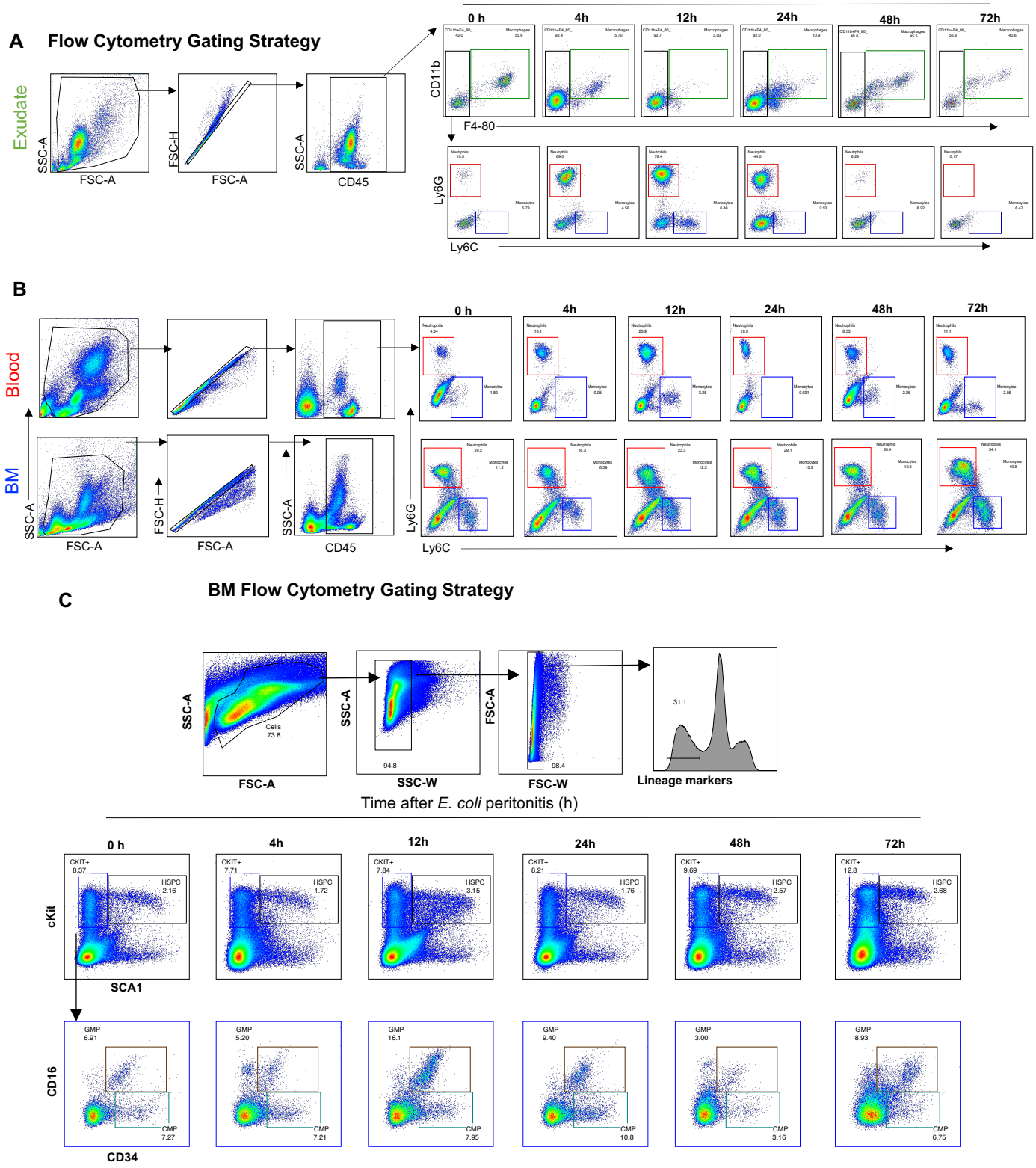

D

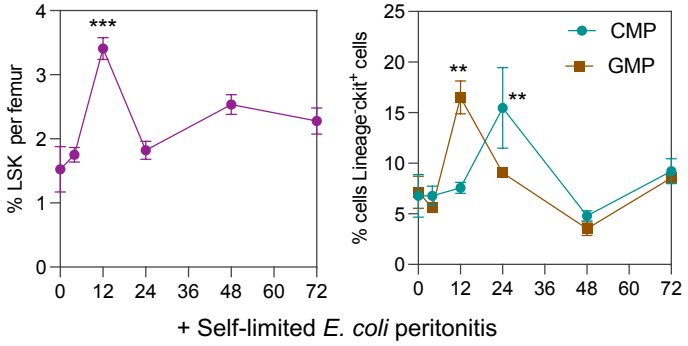

E

Mouse Bone Marrow LC-MS/MS

BM-MS/MS RvD1

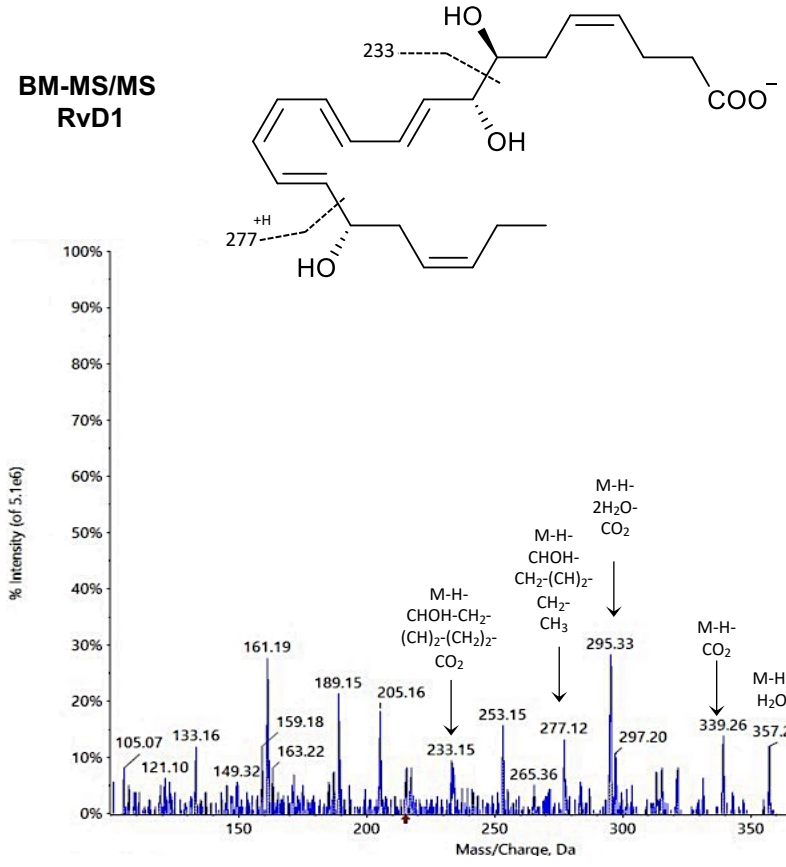

Supplemental Figure1

Mouse Bone Marrow LC-MS/MS

F

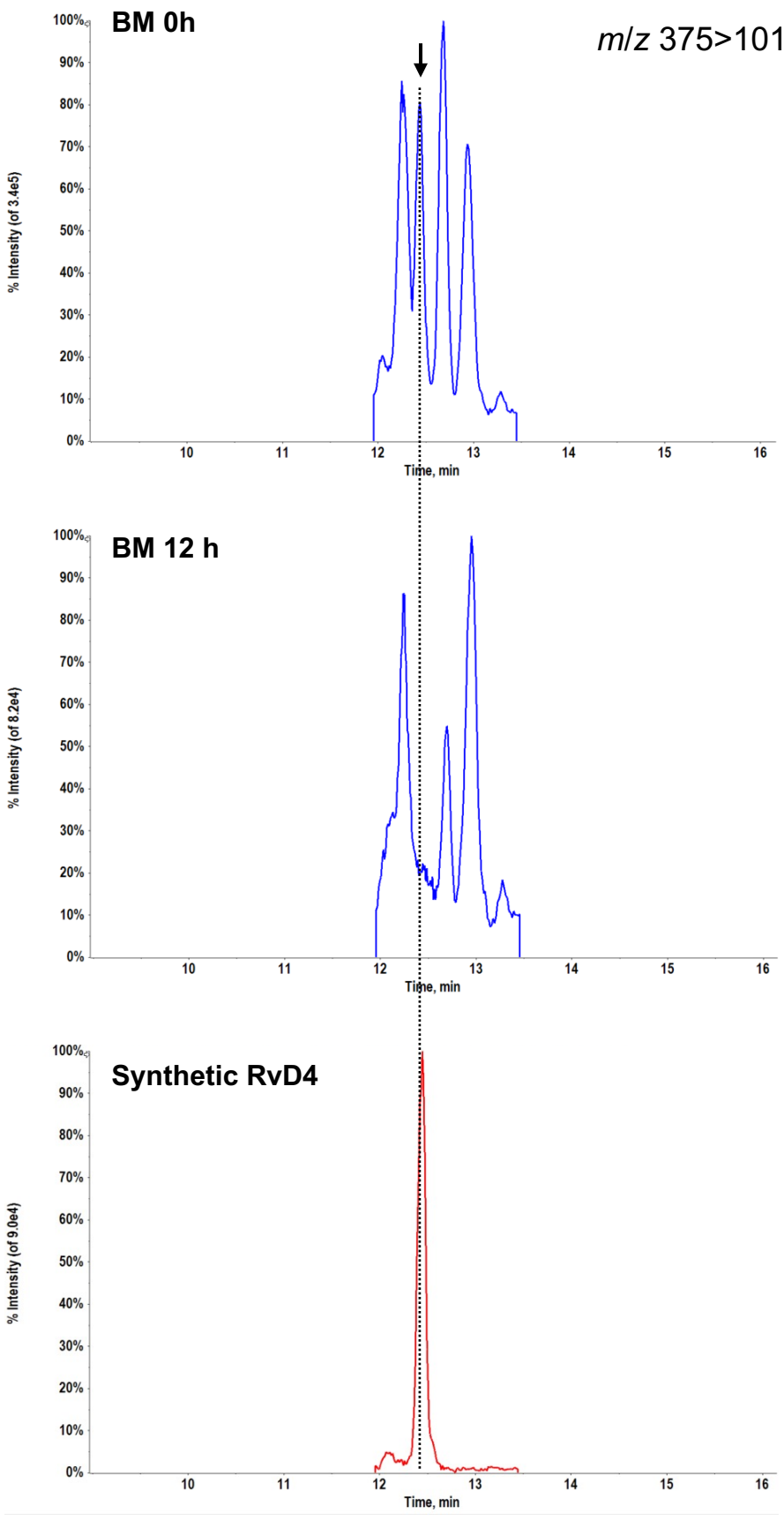

Supplemental Figure1

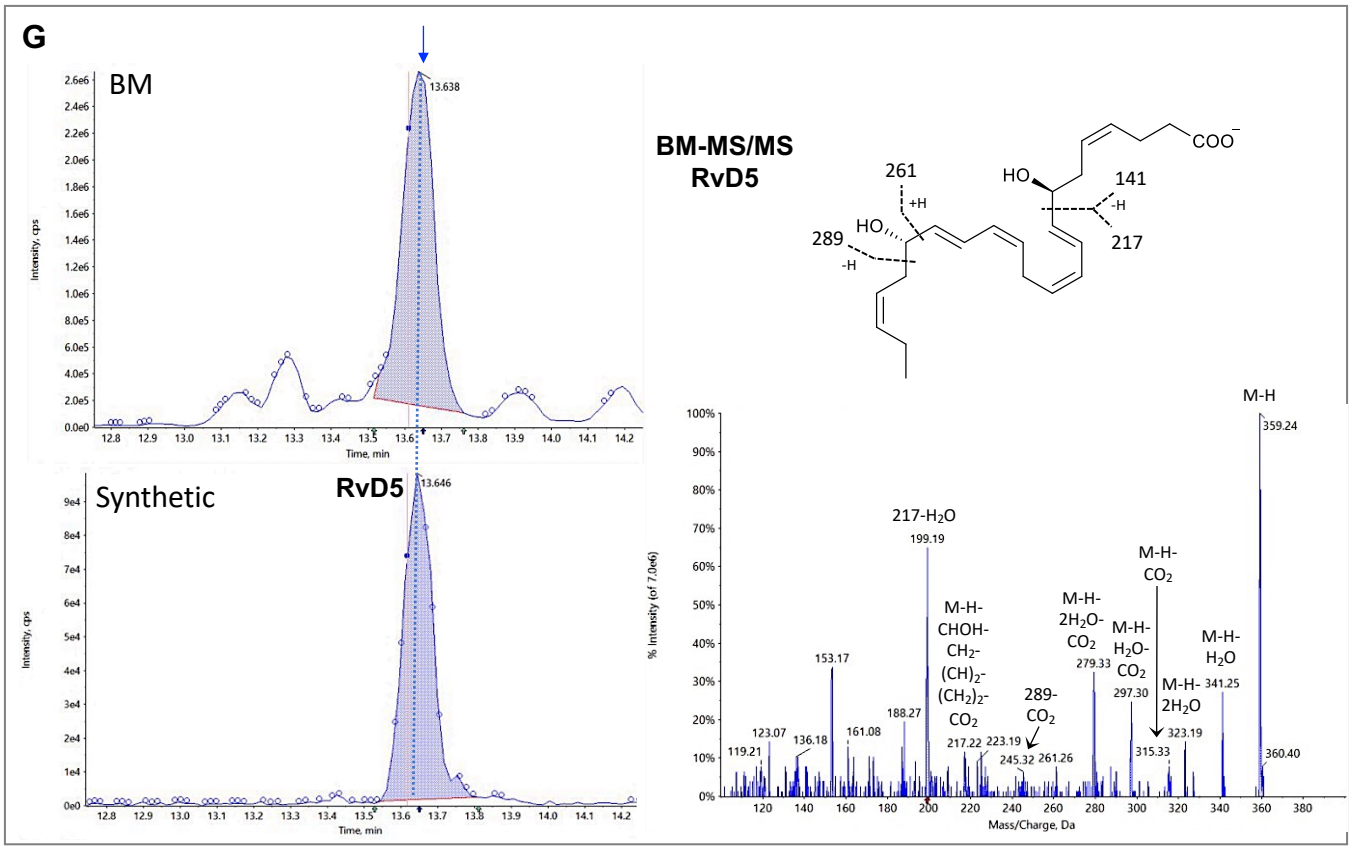

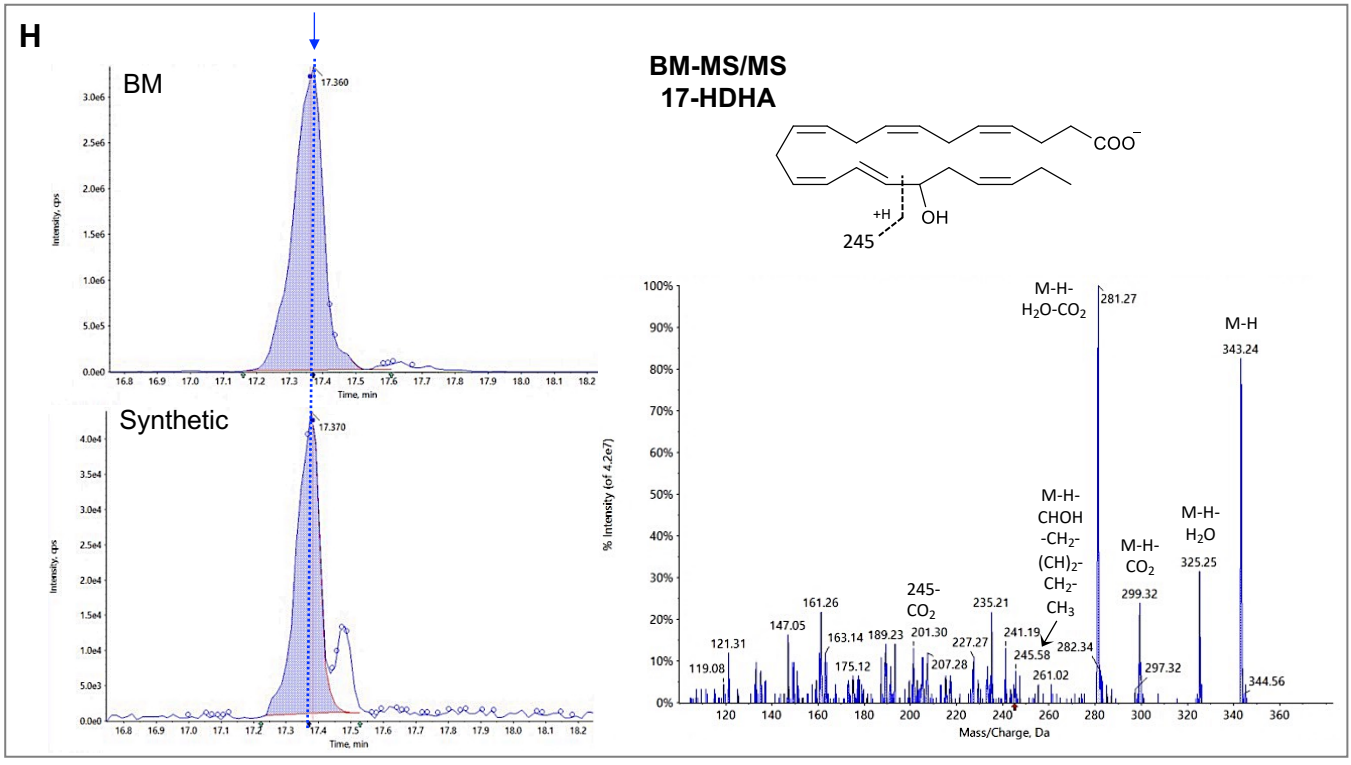

Supplemental Figure1

I

Mouse Bone Marrow LC-MS/MS

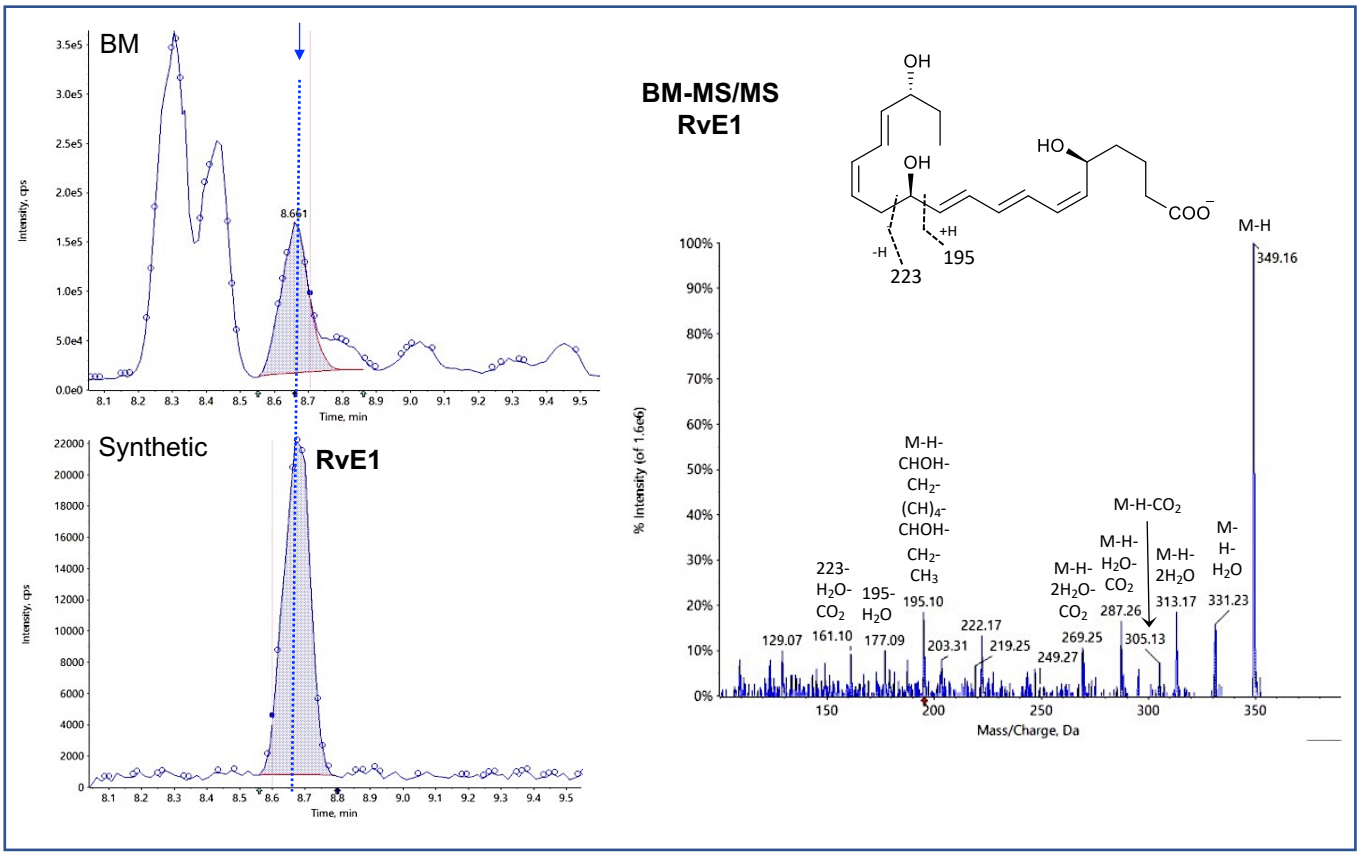

Mouse Bone Marrow LC-MS/MS

J

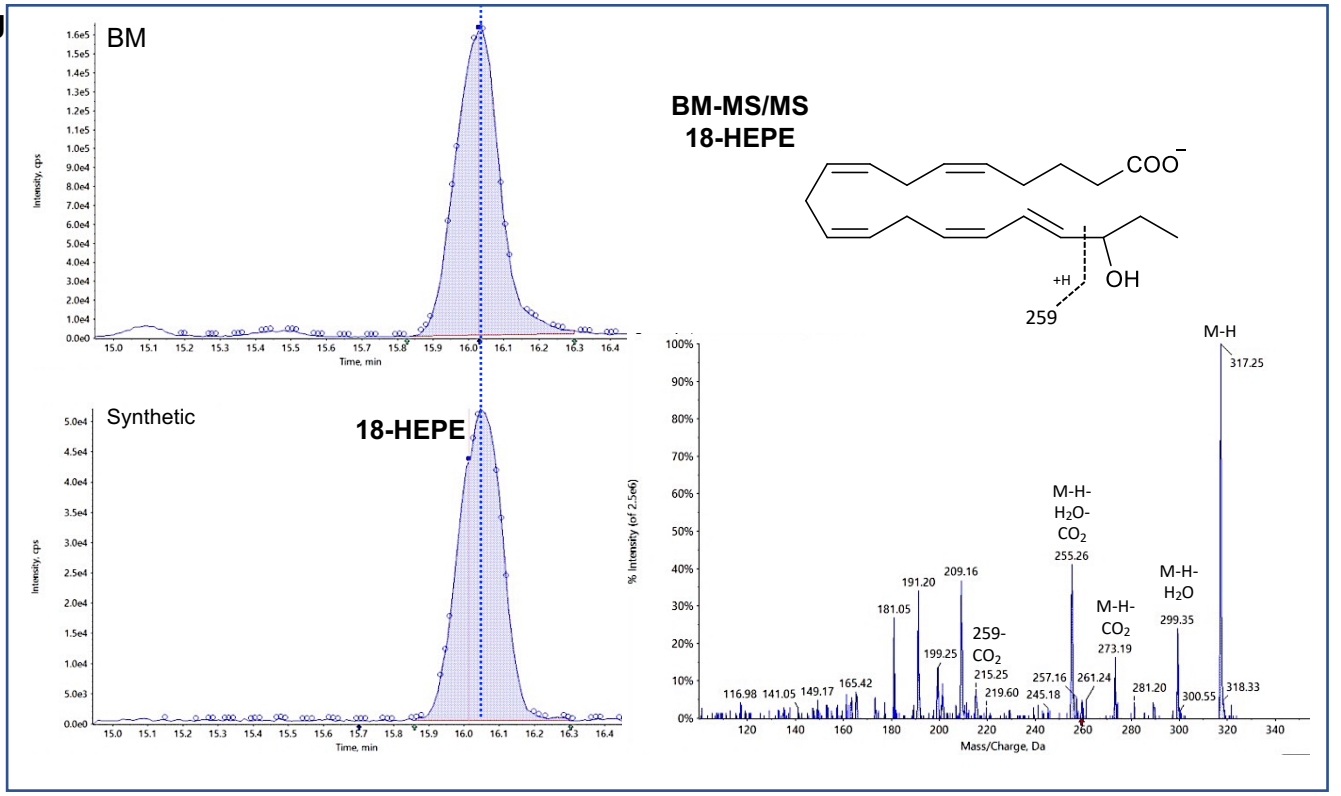

Supplemental Figure1

Mouse Blood LC-MS/MS

K

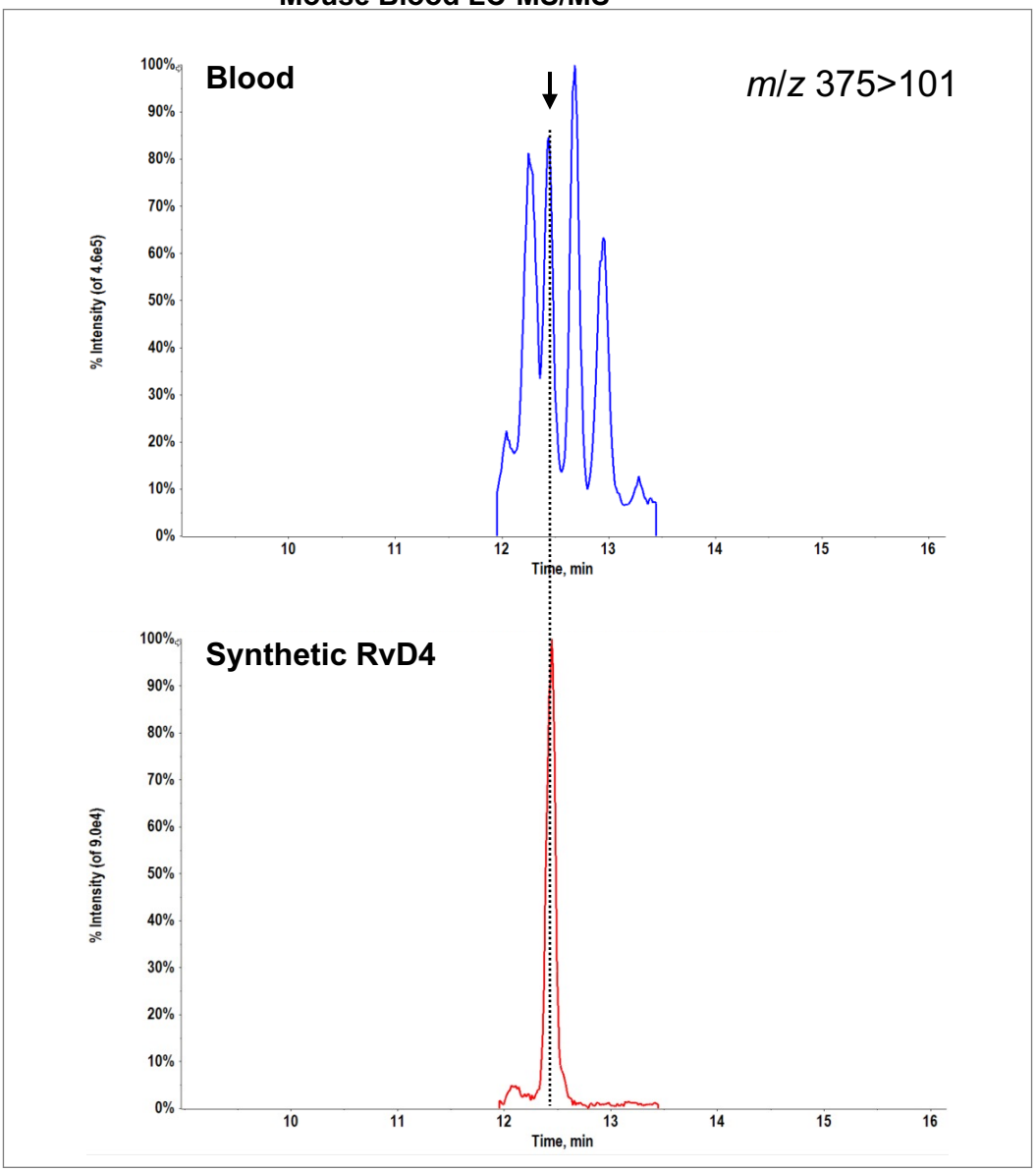

L

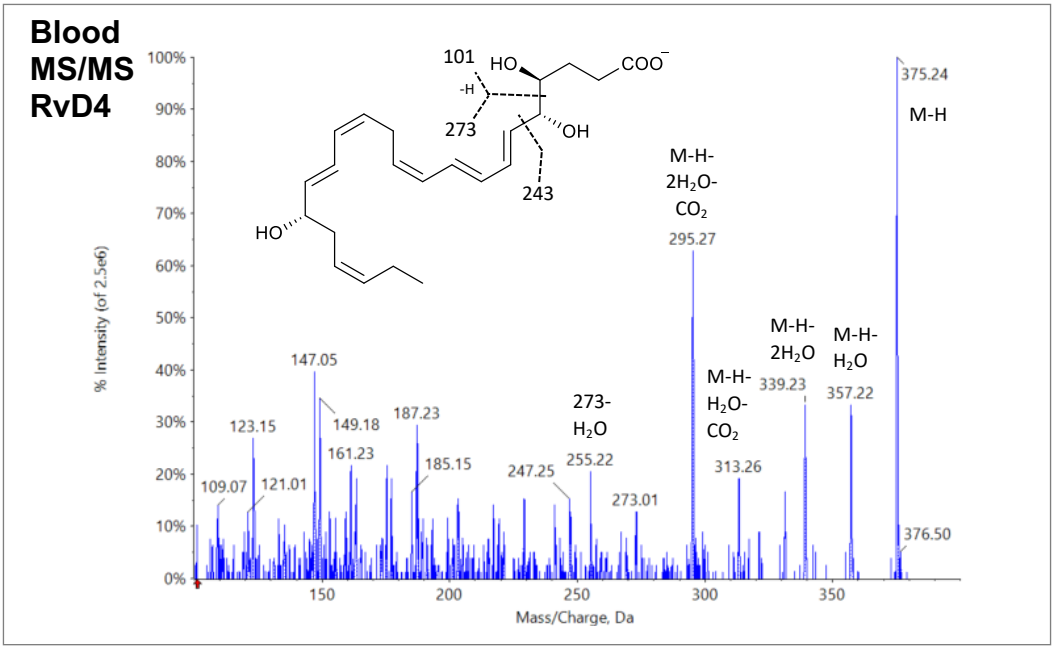

Supplemental Figure1

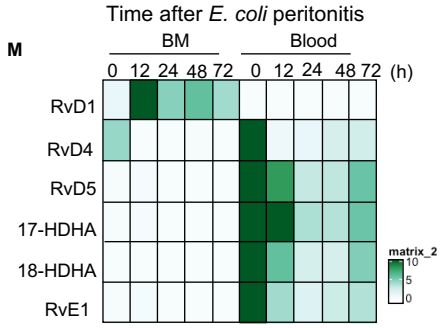

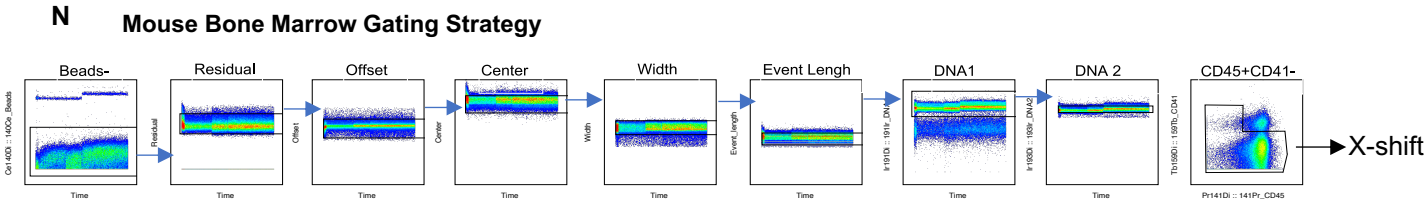

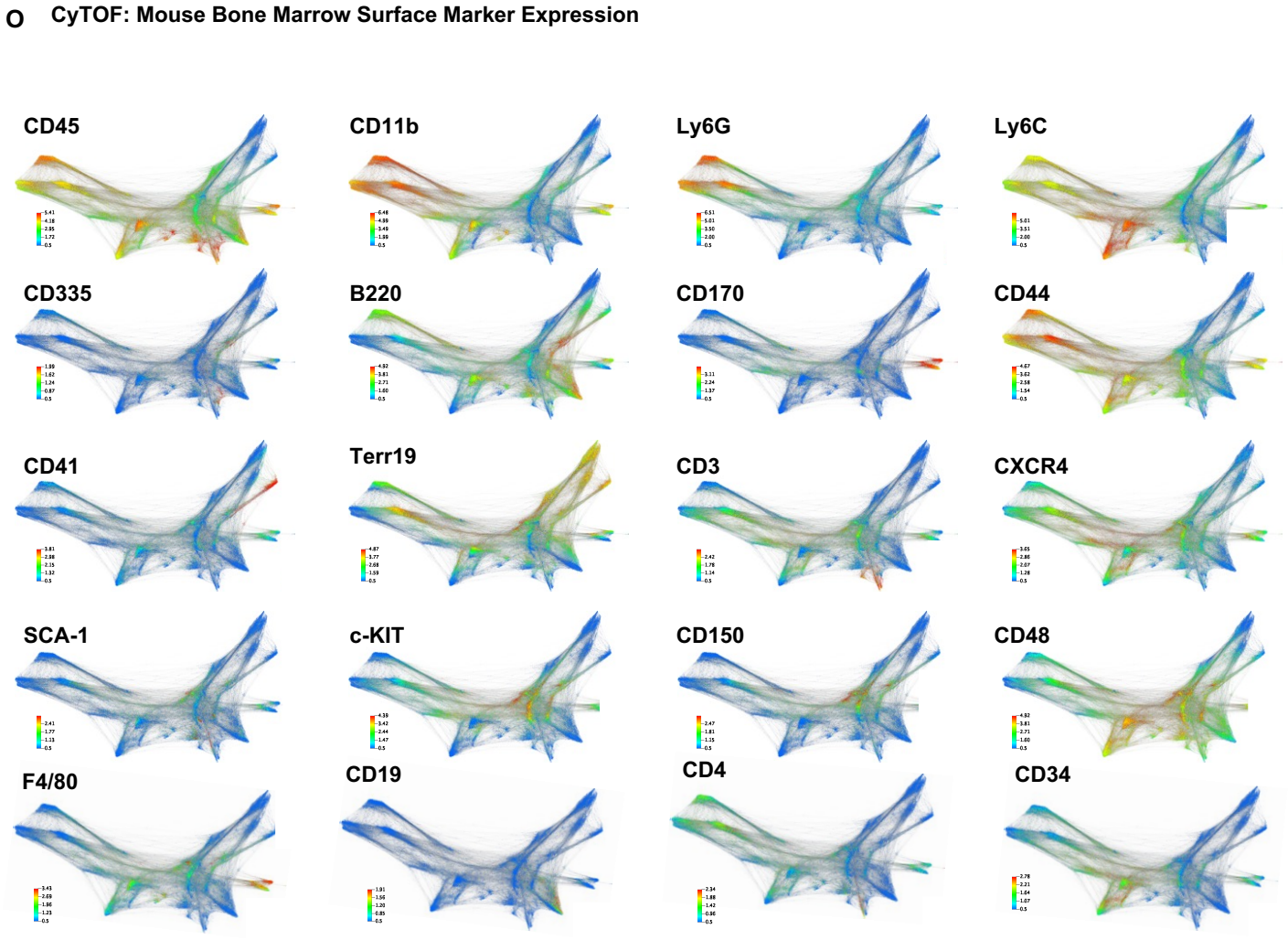

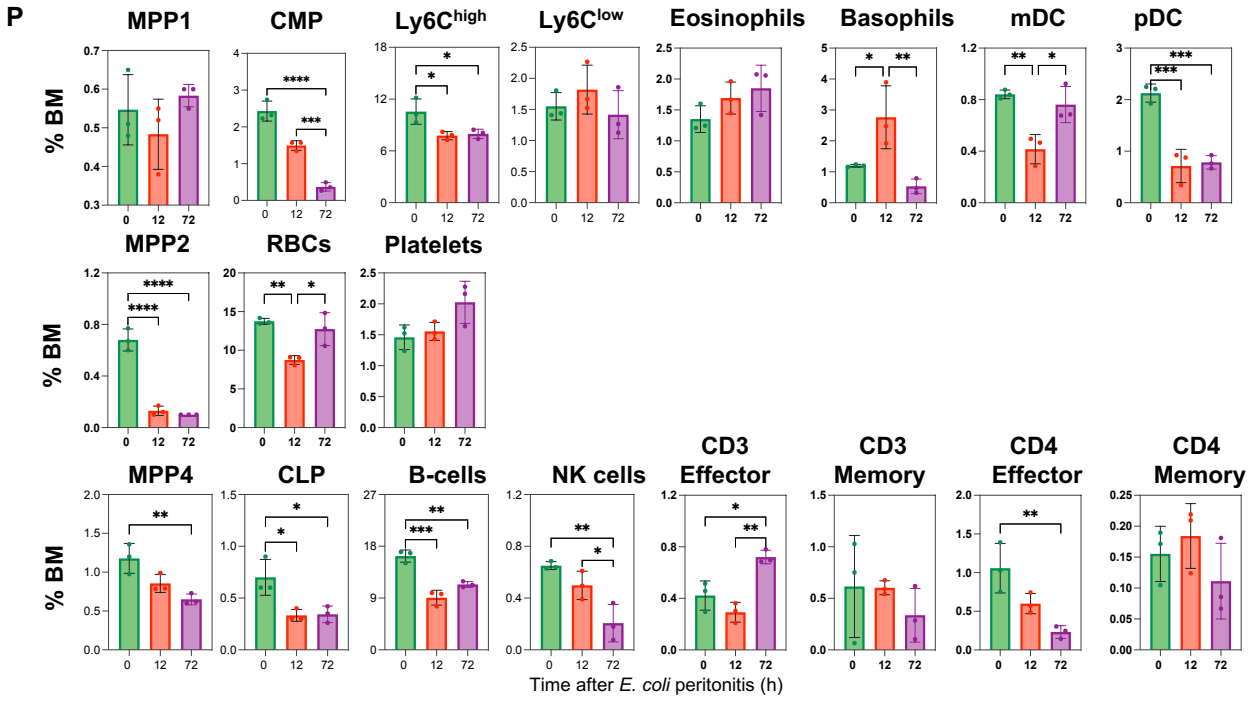

Supplemental Figure 1. Temporal production of myeloid cells and identification of RvD1, RvD5, 17-HDHA, RvE1 and 18-HEPE in mouse BM during self-limited peritonitis infections. Mice were inoculated i.p. with a self-limited dose of *E. coli* (10^5 CFU).

(A-B) Flow cytometry gating strategy used for the identification of neutrophils ($CD11b^+$ $F4/80^-$ $CD45^+Ly6G^+LyGC^-$) (Red box) and monocytes ($CD11b^+F4/80^-CD45^+Ly6G^-LyGC^+$) (blue box) in exudate, whole blood, and bone marrow. Results are means ± SEM, n=6 mice per time point.

(C) Flow cytometry gating strategy used to identify bone marrow lineage negative precursors such as LSKs ($Lineage^-SCA1^+ckit^+$), CMP (common myeloid progenitors) and GMP (granulocyte monocyte progenitor).

(D) Percent of BM-LSKs, GMPs and CMPs. Results are means ± SEM, n=6 mice per time point, *p<0.05, **p<0.01, *** p<0.001, **** p< 0.0001.

Bone marrow cells were isolated at 0, 12, 24, 48, and 72h post-inoculation for targeted LC-MS/MS metabololipidomics using a SCIEX 5500 plus. Direct Screen Captures from SciexOS-Q version 1.7.0.36606 (Analytics mode) version of:

(E) Screen Capture of BM RvD1 tandem mass spectrometry fragmentation. Inset, RvD1structure and proposed fragmentation. (See text for identification of diagnostic ions). BM RvD1 MS/MS fragmentation spectral match to the unbiased library of validated lipid mediators with fit score of 93.5% to synthetic RvD1.

(F) Screen Captures of BM RvD4 from targeted LC-MS-MS. Top: BM RvD4 at Time zero, Middle: BM RvD4 at 12h. Bottom: Synthetic RvD4. Targeted scheduled MRM in negative ion mode for m/z 375>101. MRM signal-to-noise ratio >35 in BM at 0h. Screen captures taken from Sciex OS version 1.7.036606 (Explorer Mode).

Supplemental Figure 1. Temporal production of myeloid cells and identification of RvD1, RvD5, 17-HDHA, RvE1 and 18-HEPE in mouse BM during self-limited peritonitis infections. Mice were inoculated i.p. with a self-limited dose of *E. coli* (10^5 CFU).

(G) RvD5. Left-Top: Mouse BM RvD5 , Left-Bottom: Synthetic RvD5, LC-MS/MS targeted scheduled multiple reaction monitoring (MRM) in negative ion mode for m/z 359 > 199. MRM Signal-to-noise ratio>90. Inset, RvD5 structure and proposed fragmentation. Right, RvD5 tandem mass spectrometry fragmentation from BM. BM RvD5 MS/MS fragmentation spectral match to the unbiased library of validated lipid mediators with fit score of 93.8% to synthetic RvD5.

(H) 17-HDHA. Left-Top: Mouse BM 17-HDHA, Left-Bottom: Synthetic 17-HDHA,, LC-MS/MS targeted scheduled MRM in negative ion mode for m/z 343 > 245 . MRM Signal to noise ratio> 500 Inset, 17-HDHA structure and proposed fragmentation. Right, 17-HDHA tandem mass spectrometry fragmentation from mouse BM samples. BM 17-HDHA MS/MS fragmentation spectral match to the unbiased library of validated lipid mediators with fit score of 92% to synthetic 17-HDHA.

(I) RvE1. Left-Top: Mouse BM RvE1, Left-Bottom: Synthetic RvE1, LC-MS/MS targeted scheduled MRM in negative ion mode for m/z 349 > 195. MRM Signal-to-noise ratio >50. Inset, RvE1 structure and proposed fragmentation. Right, RvE1 tandem mass spectrometry fragmentation from mouse BM samples. BM RvE1 MS/MS fragmentation spectral match to the unbiased library of validated lipid mediators with fit score of 87.5% to synthetic RvE1.

(J) 18-HEPE. Left-Top: Mouse BM 18-HEPE, Left-Bottom: Synthetic 18-HEPE, LC-MS/MS scheduled targeted MRM in negative ion mode for m/z 317 > 259. MRM Signal-to-noise ratio>300. Inset, 18-HEPE structure and proposed fragmentation. Right, 18-HEPE tandem mass spectrometry fragmentation from mouse BM samples. BM 18-HEPE MS/MS fragmentation spectral match to the unbiased library of validated lipid mediators with fit score of 92.5% to synthetic 18-HEPE.

(K) Screen Captures of BM RvD4 from targeted LC-MS-MS. Top: Blood RvD4. Bottom: Synthetic RvD4. Targeted scheduled MRM in negative ion mode for m/z 375>101. MRM signal-to-noise ratio >42. Screen captures taken from Sciex OS version 1.7.036606 (Explorer Mode).

(L) Screen Capture of BM RvD4 tandem mass spectrometry fragmentation. Inset: RvD4 structure and proposed fragmentation. BM RvD4 MS/MS fragmentation spectral match to an unbiased library of synthetic standards with a fit score of 96.5% to synthetic RvD4. BM-RvD4 MS/MS spectra ion gave an of *m/z* 375 = M-H and daughter ions of *m/z* 357 = M-H-H_2O, 339 = M-H-$2H_2O$, 313 = M-H-H_2O-CO_2, 295 = M-H-$2H_2O$-CO_2, 255 = 273-H_2O and 101= M-H-CHOH-$(CH)_6$-CH_2-$(CH)_4$-CHOH-CH_2-$(CH)_2$-CH_2-CH_3

Note that the accuracy for data acquisition of the Sciex 5500 is 0.1 amu; the additional digits in the screen captures are the default setting (the digit [amu] in the 2nd decimal place does not accurately reflect the mass of the ions).

(H-J) Screen Captures of targeted LC-MS/MS metabololipidomics using a SCIEX 5500 plus. Direct Screen Captures from SciexOS-Q version 1.7.0.36606 (Analytics mode) version.

Supplemental Figure 1. Temporal production of myeloid cells and identification of RvD1, RvD5, 17-HDHA, RvE1 and 18-HEPE in mouse BM during self-limited peritonitis infections. Mice were inoculated i.p. with a self-limited dose of *E. coli* (10^5 CFU).

(M) HeapMAP of mean of fold change in the abundance of Resolvins identified in the BM and whole blood during self-limited infections at indicated times. Results of whole blood samples were pooled from 3 mice in each time point.

(N) CyTOF: BM cells were isolated at 0hr, 12hr, and 72hr from mice with peritonitis. Gating strategy used for X-shift analysis.

(O) CyTOF: $CD45^{+}CD41^{-}$ single cells Force directed layout map (Vortex) showing (94,500 total single cells) cluster by x-shift (n=3 mice per time point (~10,500 per mouse) surface markers expression).

(P) CyTOF**:** Percent of BM immune populations such as eosinophils, plasmacytoid and monocytic dendritic cell (pDC and mDC), and lymphocytes. Results are means $\pm$ SEM, n=3 mice per time point. *p<0.05, **p<0.01, *** p<0.001, **** p< 0.0001. 0hr vs. 12hr or 72hr. Statistical analysis was carried out using 2-way ANOVA with Tukey's multiple comparisons test.

Reference:

Serhan CN, Clish CB, Brannon J, Colgan SP, Chiang N, Gronert K. Novel functional sets of lipid-derived mediators with antiinflammatory actions generated from omega-3 fatty acids via cyclooxygenase 2-nonsteroidal antiinflammatory drugs and transcellular processing. J Exp Med. 2000 Oct 16;192(8):1197-204. doi: 10.1084/jem.192.8.1197. PMID: 11034610; PMCID: PMC2195872.

Serhan CN, Hong S, Gronert K, Colgan SP, Devchand PR, Mirick G, Moussignac RL. Resolvins: a family of bioactive products of omega-3 fatty acid transformation circuits initiated by aspirin treatment that counter proinflammation signals. J Exp Med. 2002 Oct 21;196(8):1025-37. doi: 10.1084/jem.20020760. PMID: 12391014; PMCID: PMC2194036.

Arita M, Oh SF, Chonan T, Hong S, Elangovan S, Sun YP, Uddin J, Petasis NA, Serhan CN. Metabolic inactivation of resolvin E1 and stabilization of its anti-inflammatory actions. J Biol Chem. 2006 Aug 11;281(32):22847-54. doi: 10.1074/jbc.M603766200. Epub 2006 Jun 6. PMID: 16757471.

Sun, Y.P., Oh, S.F., Uddin, J., Yang, R., Gotlinger, K., Campbell, E., Colgan, S.P., Petasis, N.A., and Serhan, C.N. (2007). Resolvin D1 and its aspirin-triggered 17R epimer. Stereochemical assignments, anti-inflammatory properties, and enzymatic inactivation. J Biol Chem *282*, 9323-9334. 10.1074/jbc.M609212200.

Chiang N, Fredman G, Bäckhed F, Oh SF, Vickery T, Schmidt BA, Serhan CN. Infection regulates pro-resolving mediators that lower antibiotic requirements. Nature. 2012 Apr 25;484(7395):524-8. doi: 10.1038/nature11042. PMID: 22538616; PMCID: PMC3340015.

Winkler, J.W., Libreros, S., De La Rosa, X., Sansbury, B.E., Norris, P.C., Chiang, N., Fichtner, D., Keyes, G.S., Wourms, N., Spite, M., and Serhan, C.N. (2018). Structural insights into Resolvin D4 actions and further metabolites via a new total organic synthesis and validation. J Leukoc Biol. 10.1002/JLB.3MI0617-254R.

Supplemental Figure2

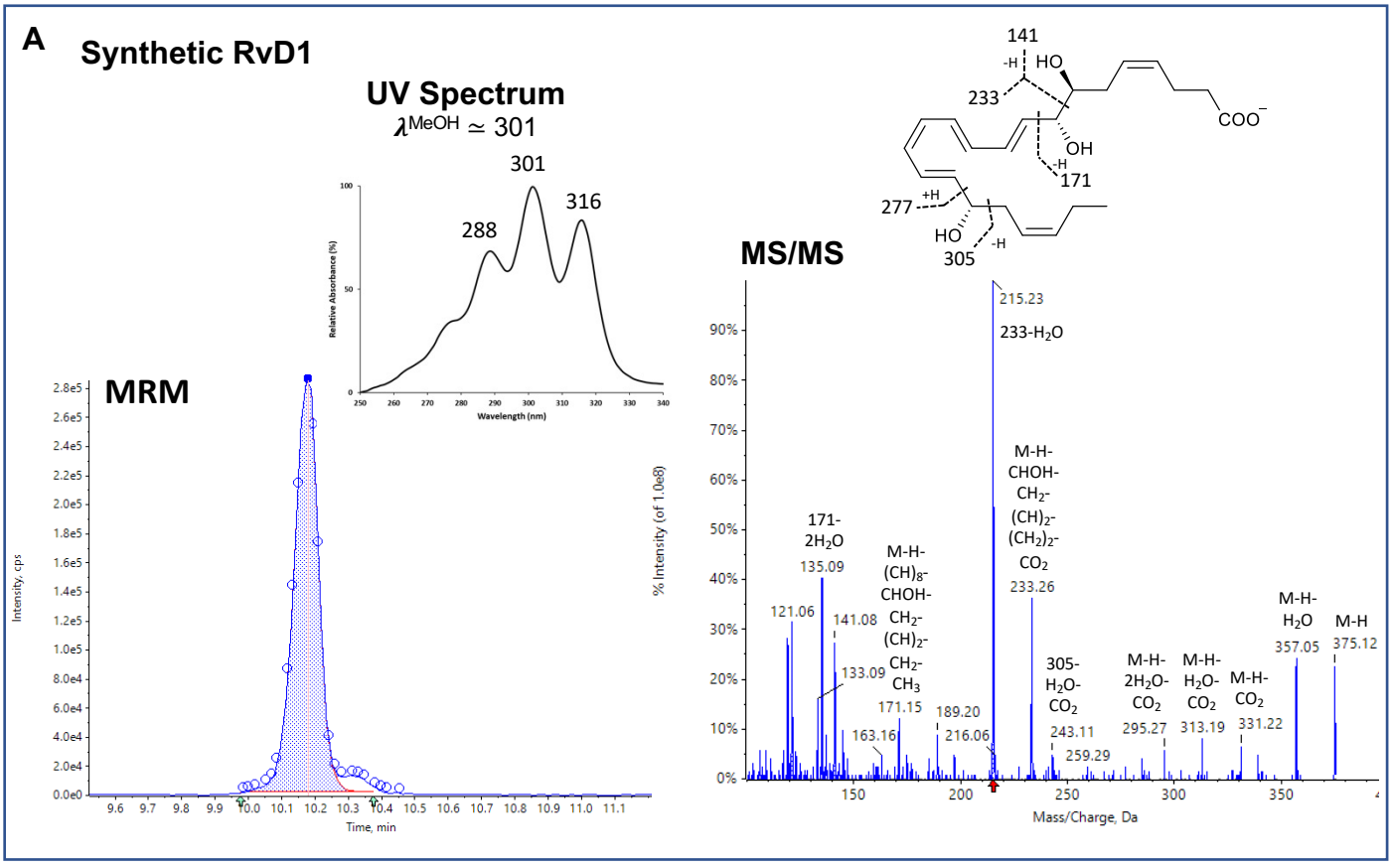

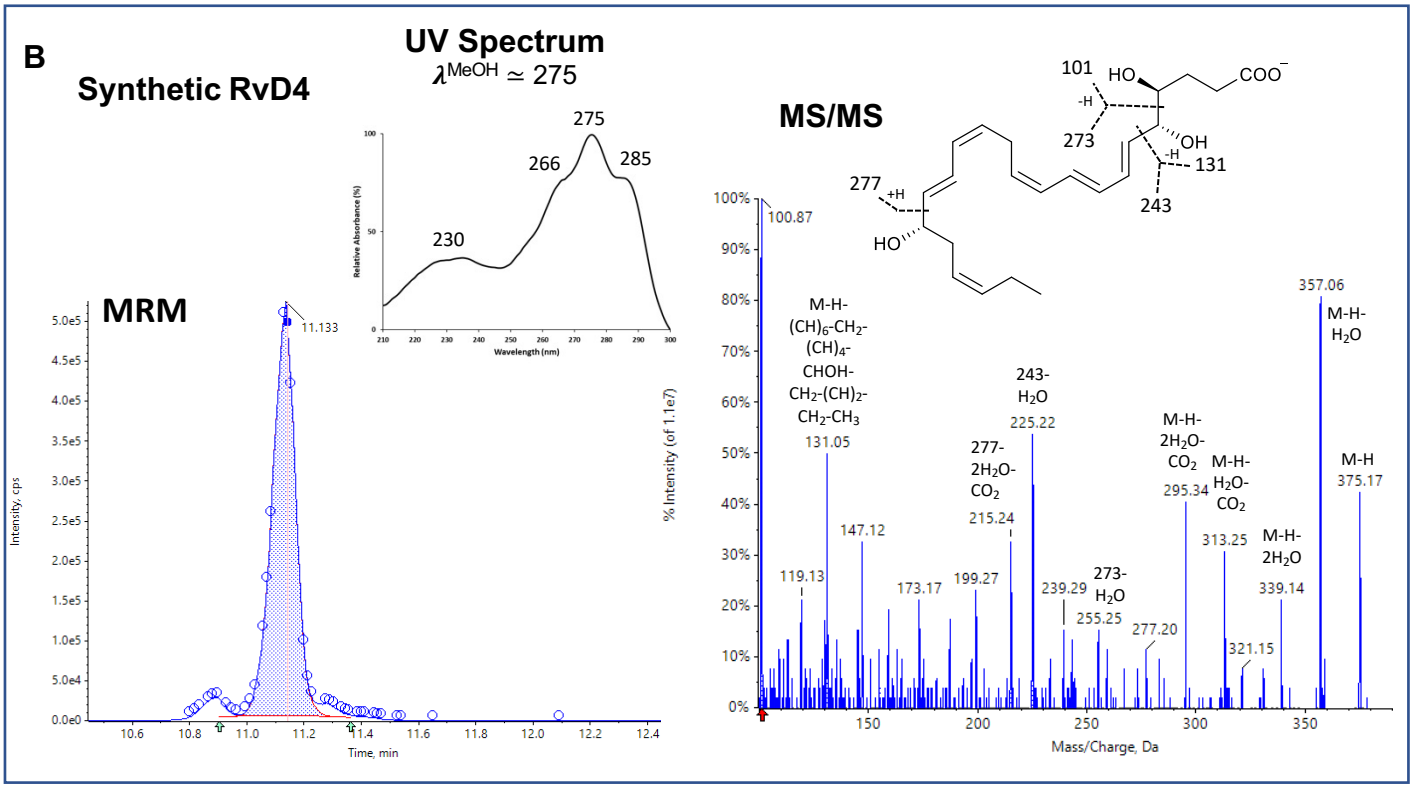

Supplemental Figure 2

C **CyTOF: Bone Marrow Surface Expression**

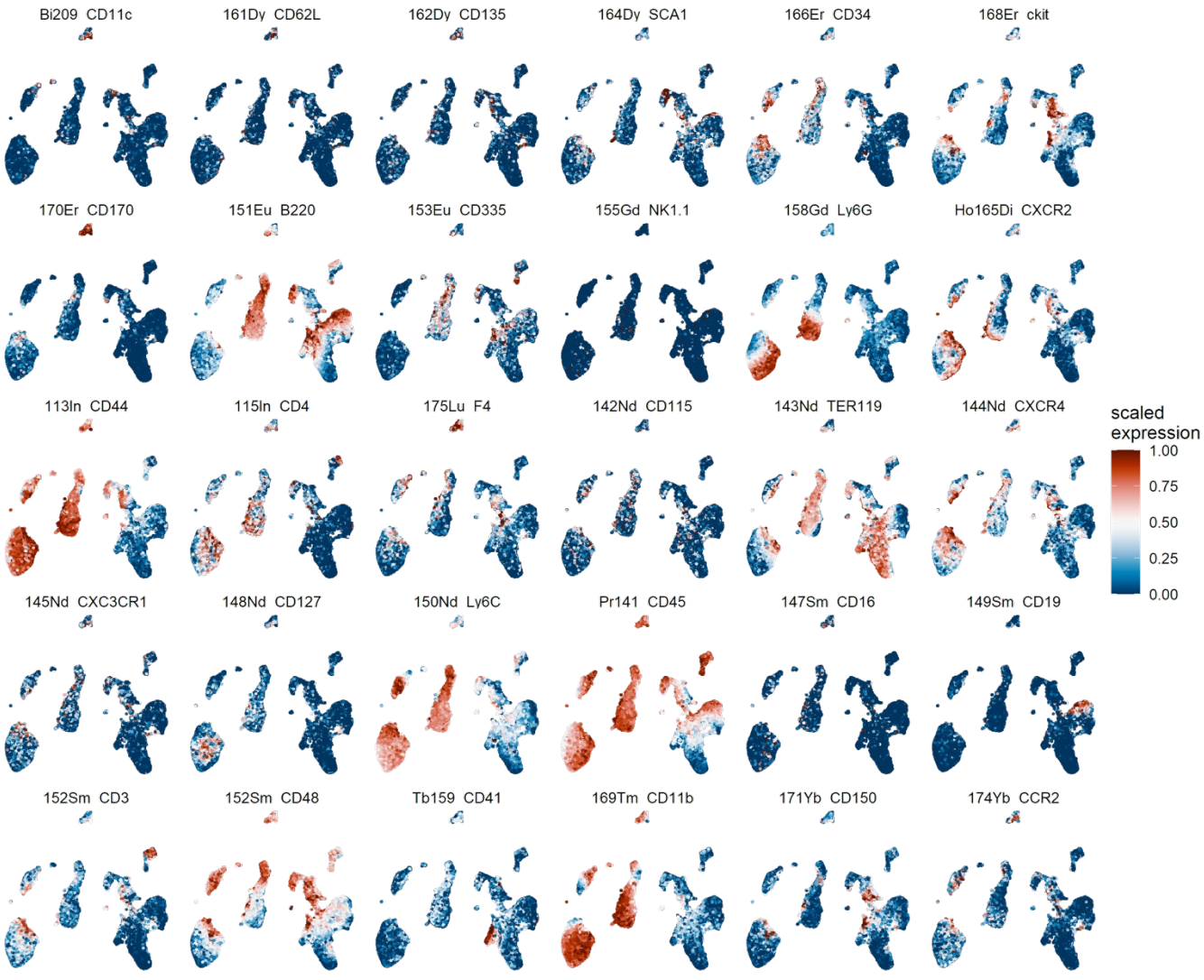

D

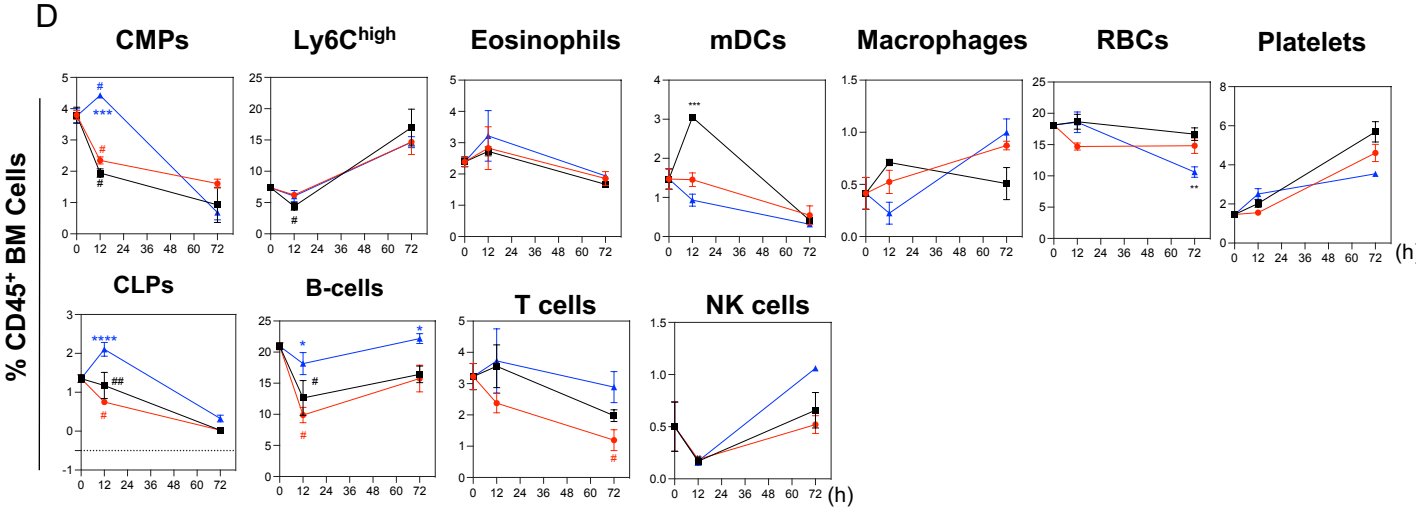

+Self-limited *E. coli* peritonitis

Supplemental Figure2

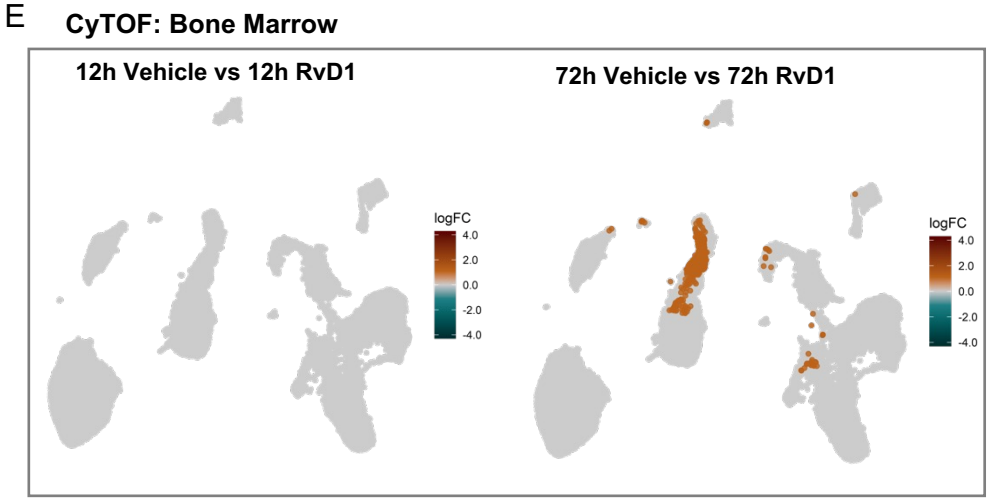

Supplemental Figure 2. RvD1 and RvD4 differently regulate BM myeloid cells at the single-cell level. Mice inoculated with *E. coli (*10^5 CFU, i.p.) were also (i.v.) administered RvD1 (100ng/mouse), RvD4 (100ng/mouse) or vehicle alone (0.01% vol/vol *ethanol* in saline). BM cells were collected at 0h, 12h and 72h.

(A) Authentication of synthetic Resolvin D1. *Left*, Targeted multiple reaction monitoring (MRM) for *m*/*z* 375 > 215 (RvD1) with a retention time (T_R) = 10.18 min. *Inset*: UV absorption spectrum with λ_{max}^{MeOH} = 301 nm. *Right*, Tandem mass spectrometry spectrum and proposed fragmentation of RvD1, with an unbiased matching score of 99.4% to synthetic RvD1 contained in our custom spectral library of authentic reference standards. Screen captures taken from Sciex OS version 1.7.036606. UV data were acquired on an Agilent 8453 UV-vis spectrophotometer.

(B) Authentication of synthetic Resolvin D4. *Left*, MRM for *m*/*z* 375 > 101 (RvD4) with a retention time (T_R) = 11.13 min. *Inset*: UV absorption spectrum of RvD4 with λ_{max}^{MeOH} = 275 nm. *Right*, Tandem mass spectrometry spectrum of RvD4 and its proposed structure fragmentations with a matching fit score of 99.7%. Screen captures taken from Sciex OS version 1.7.036606. UV data were obtained using an Agilent 8453 UV-vis spectrophotometer.

(A-B) Note that the accuracy for data acquisition of the Sciex 6500 plus is 0.1 amu; the additional digits in the screen captures are the default setting (the digit [amu] in the 2nd decimal place does not accurately reflect the mass of the ions.)

(C) UMAPs of surface markers used to identify BM immune populations.

(D) Percent frequency of BM immune populations. Results are means ± SEM, n=3 mice per time point. 0hr vs. 12hr and 72hr: # p<0.05 ##p<0.01. Resolvins (RvD1 or RvD4) vs. *E. coli* + vehicle, *p<0.05, **p<0.01, *** p<0.001. Statistical analysis was carried out using two-way ANOVA with Tukey's multiple comparisons test.

(E) UMAPs showing logFC change between *E. coli* + RvD1 vs. *E. coli* + vehicle calculated using edgeR with diffcyt. (E-F) Only statistically significant populations were colored (p<0.05) and adjusted using a Benjamini-Hochberg correction.

Reference:

Sun, Y.P., Oh, S.F., Uddin, J., Yang, R., Gotlinger, K., Campbell, E., Colgan, S.P., Petasis, N.A., and Serhan, C.N. (2007). Resolvin D1 and its aspirin-triggered 17R epimer. Stereochemical assignments, anti-inflammatory properties, and enzymatic inactivation. J Biol Chem *282*, 9323-9334. 10.1074/jbc.M609212200.

Winkler, J.W., Libreros, S., De La Rosa, X., Sansbury, B.E., Norris, P.C., Chiang, N., Fichtner, D., Keyes, G.S., Wourms, N., Spite, M., and Serhan, C.N. (2018). Structural insights into Resolvin D4 actions and further metabolites via a new total organic synthesis and validation. J Leukoc Biol. 10.1002/JLB.3MI0617-254R.

Supplemental Figure3

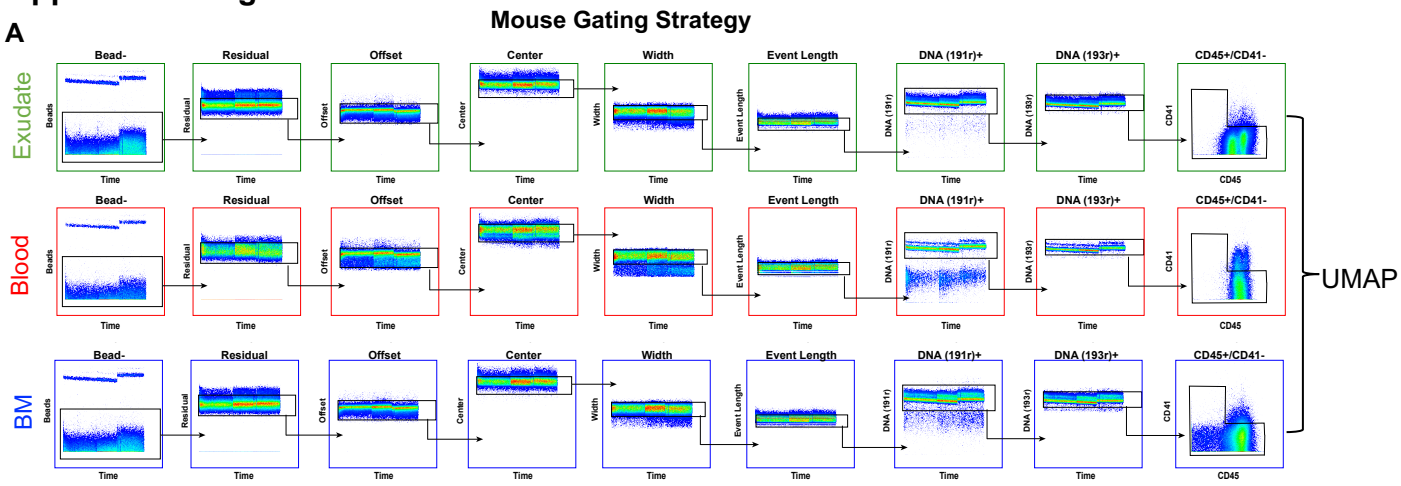

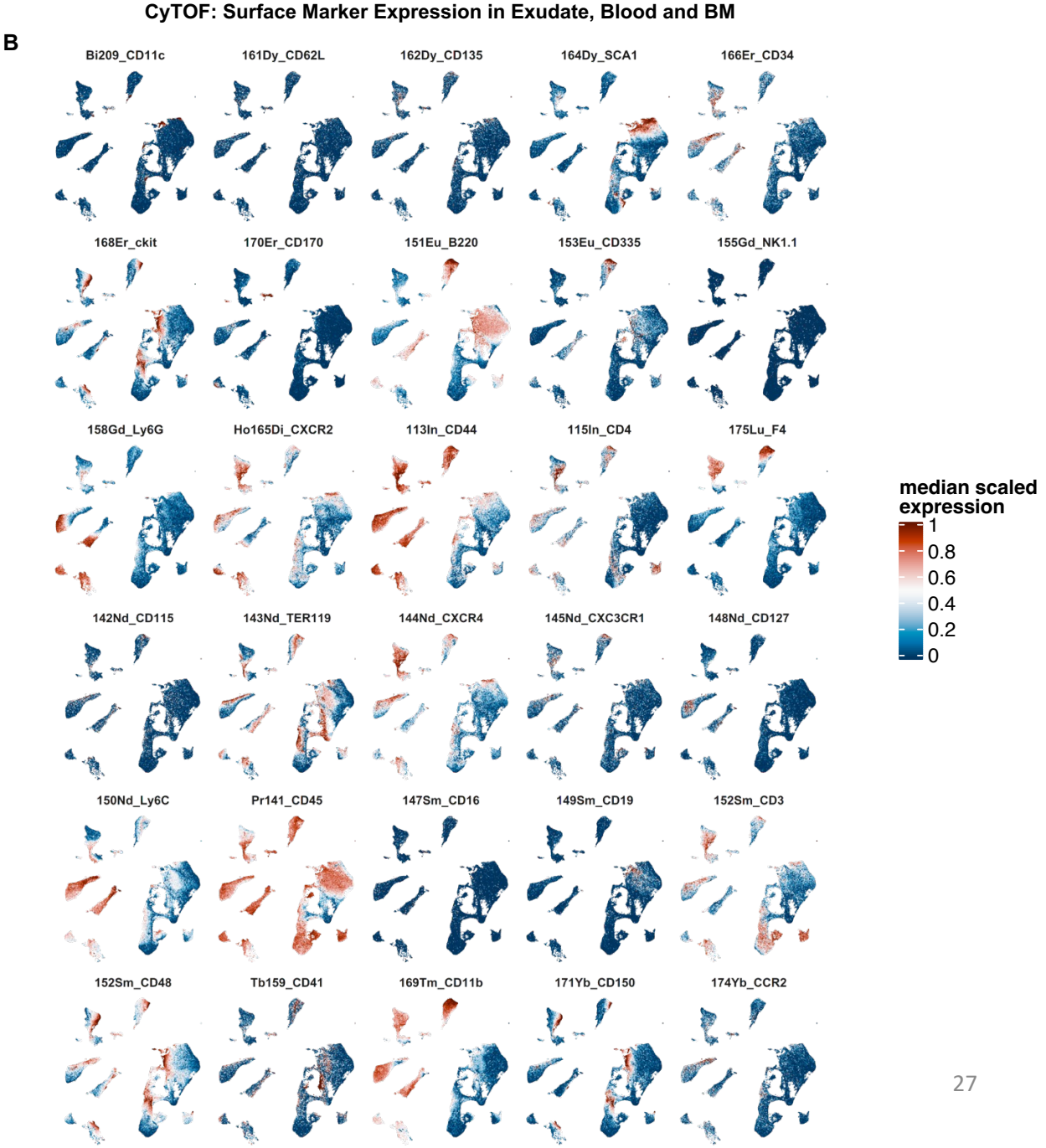

Supplemental Figure 3

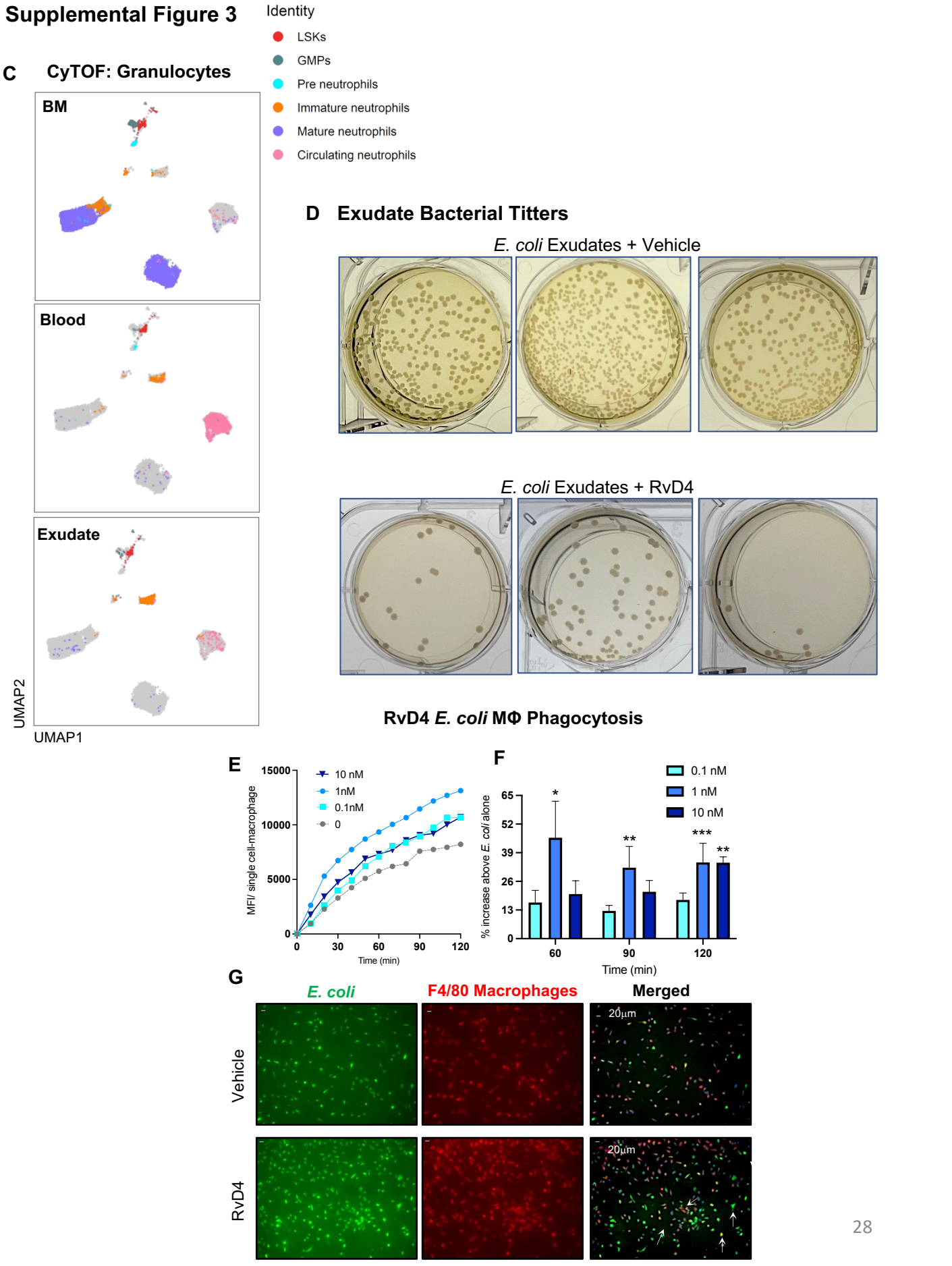

Supplemental Figure 3. RvD4 regulates neutrophils during self-limited infections and increases *E. coli* phagocytosis by macrophages. Mice inoculated with *E. coli (*10^5 CFU, i.p.) were also (i.v.) administered RvD1 (100ng/mouse), RvD4 (100ng/mouse) or vehicle alone (0.01% *vol/vol* ethanol in saline). Exudates, whole blood, and BM cells were collected at 0h, 12h and 72h.

(A) CyTOF: Gating strategy of mouse exudates, whole blood, and BM cells for UMAP analysis.

(B) CyTOF: UMAPs of surface expression

(C) CyTOF: Compartment-specific UMAP of neutrophil populations in exudate, blood, and BM.

(D) Representative photographs of bacterial titers from infectious exudates of n=4-5 mice per group.

(E-G) Peritoneal macrophages were plated onto chamber slides ($1x10^5$ cells/well) and incubated with RvD4 (0.1nM, 1nM or 10 nM) or vehicle control (0.01% ethanol *vol/vol*) for 15 min at 37°C followed by addition of BacLight Green labeled live *E. coli* to initiate phagocytosis.

(E) Mean fluorescence intensity (MFI)/cell of 5 fields/well from 0-120 min from one representative experiment.

(F) Percent increase of phagocytosis compared to *E. coli* alone, *$p<0.05$, ** $p<0.01$, ***$p<0.001$, unpaired two-tailed t-test. Results are means ± SEM, n=6 mice per condition.

(G) Representative fluorescent images of *E. coli* (Green), surface staining macrophage surface marker-F4/80 (Red), and merged images with DAPI staining in blue. Scale bars: 20μm.

Supplemental Figure 4

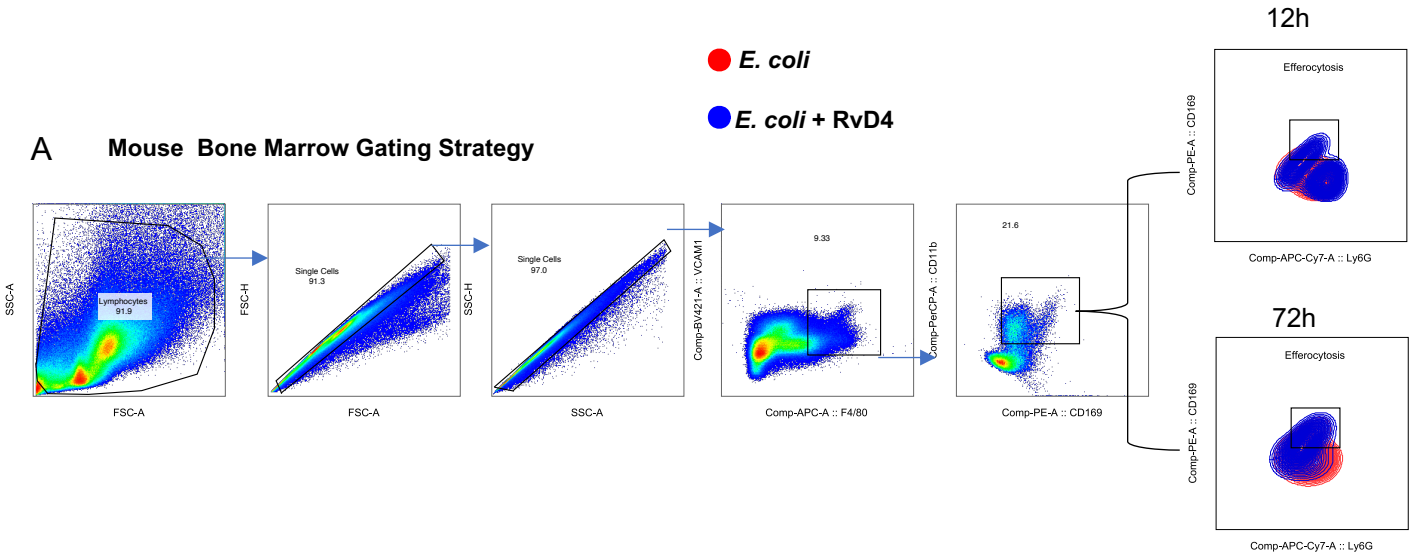

B Macrophage Efferocytosis Confocal Microscopy

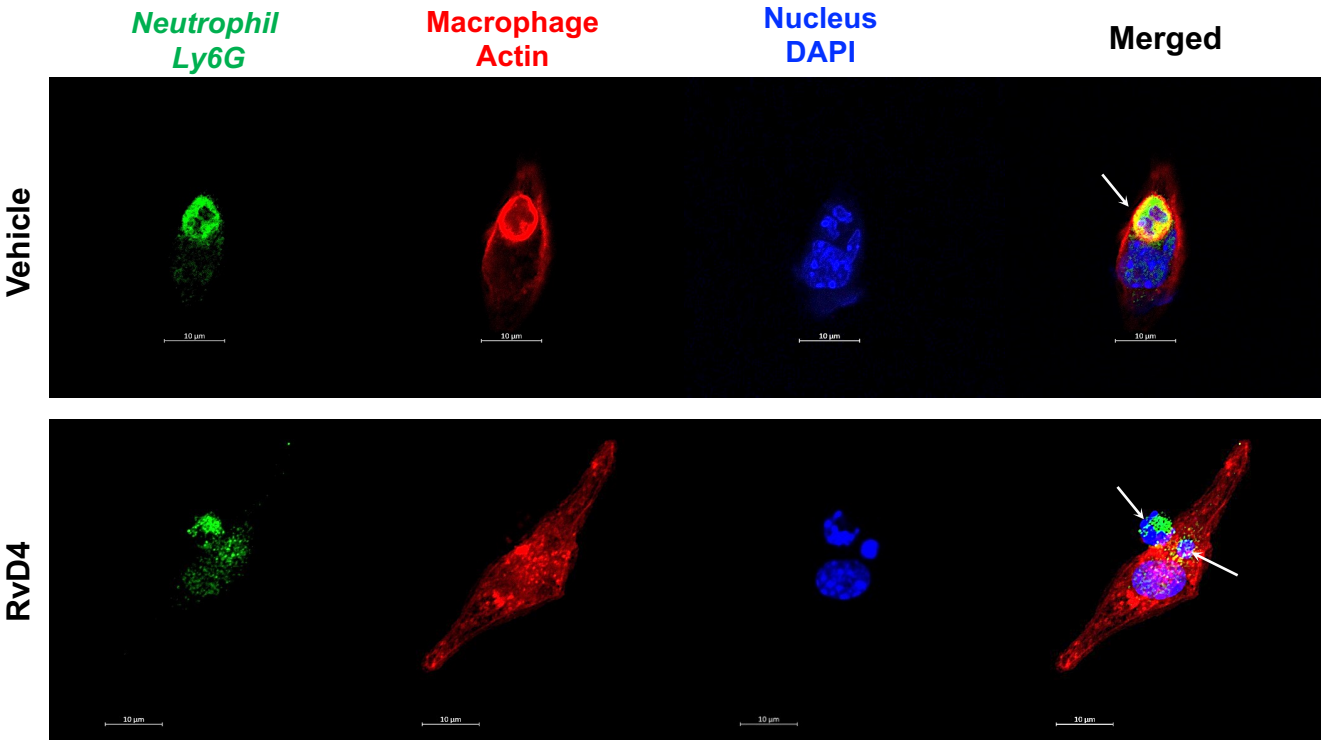

Supplemental Figure 4

C

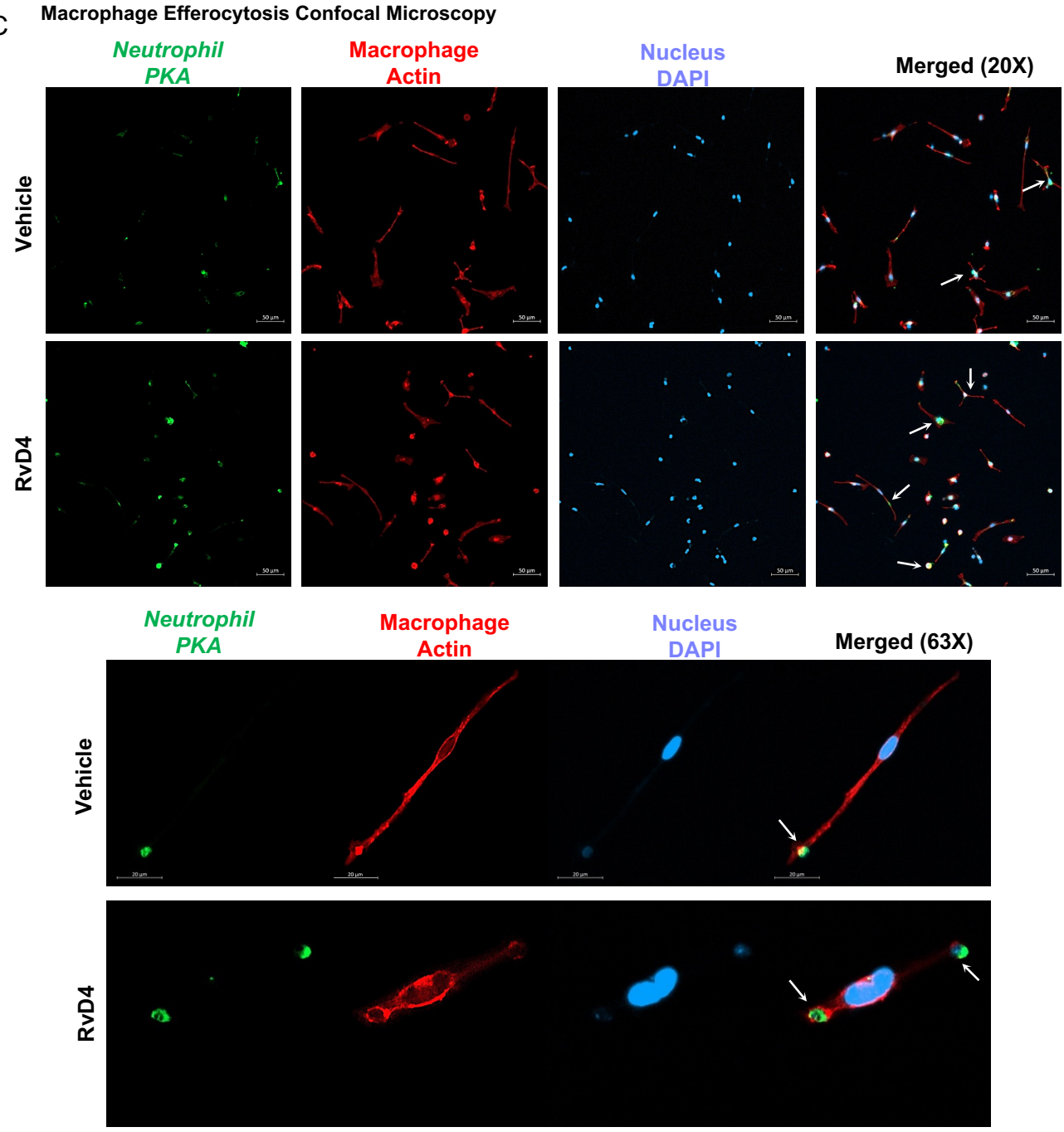

Supplemental Figure 4. RvD4 increases BM macrophage efferocytosis of BM aged neutrophils.

(A) Flow cytometry gating strategy used to identify BM CD169^{+} macrophages (CD169^{+}VACAM1^{+}F4/80^{+}CD11b^{+}) efferocytosis of neutrophils (Ly6G^{+}).

(B-C) BM-derived macrophages (1×10^{5} cells) were seeded on gelatin-coated glass coverslips in a 12-well plate for 24hrs. MΦ were treated with 1nM of RvD4 or vehicle control (0.01% ethanol vol/vol) 15 minutes prior to addition of purified apoptotic BM neutrophils (1:5 M2: aged neutrophil). Confocal microscopy images of BM-derived macrophages (Actin) efferocytosis of senescent BM neutrophils (Ly6G or PKA label aged neutrophils). Scale bar represents 10-20um. White arrows indicate ingested apoptotic neutrophils. Representative images of n=4 BM from independent experiments.

Supplemental Figure5

A Human Bone Marrow Gating Strategy

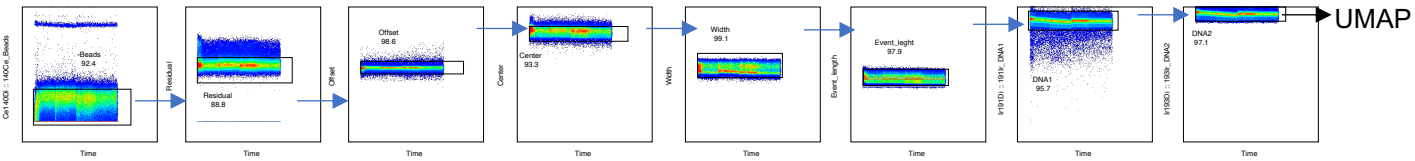

B Human Bone Surface Markers

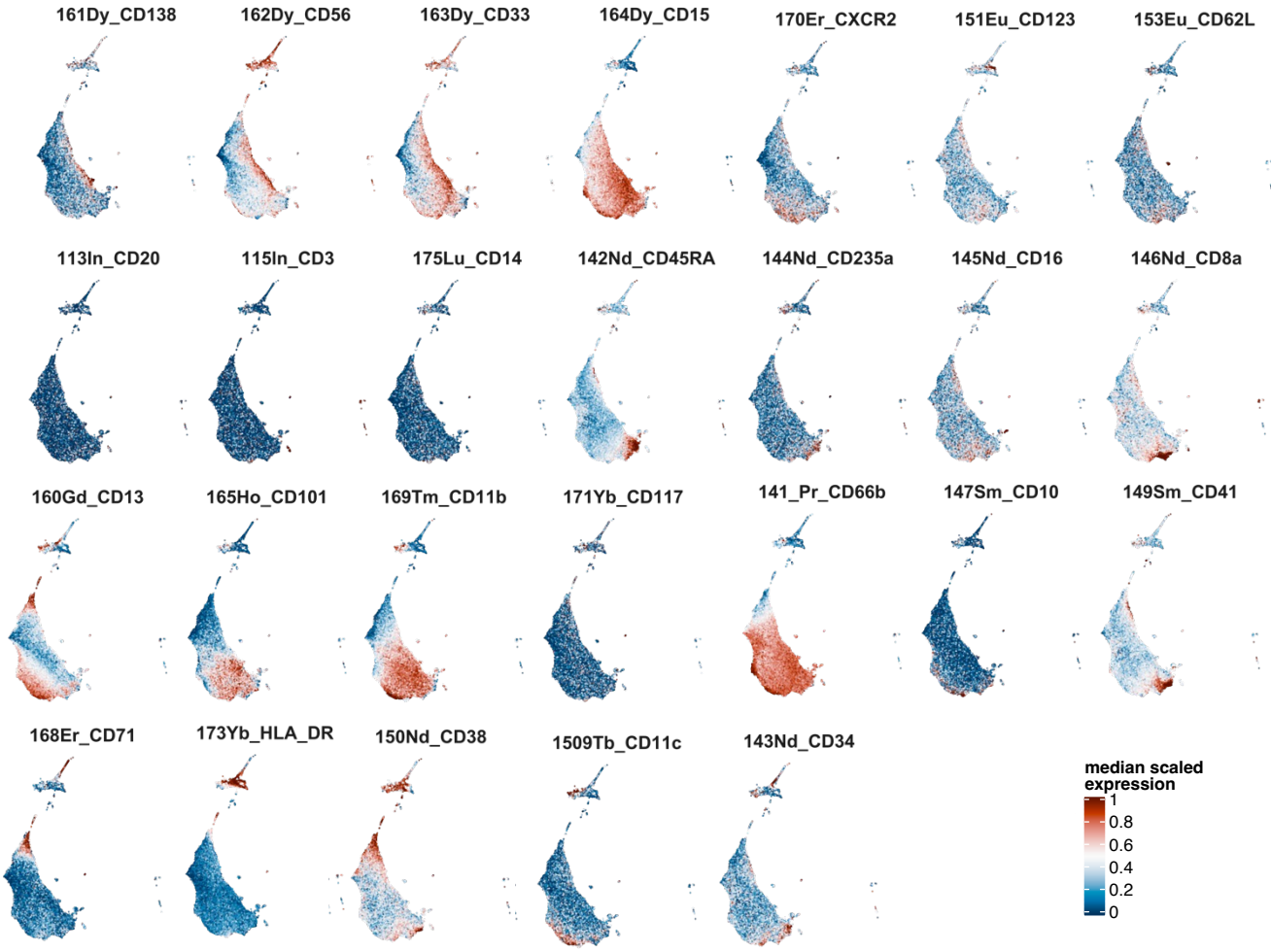

C

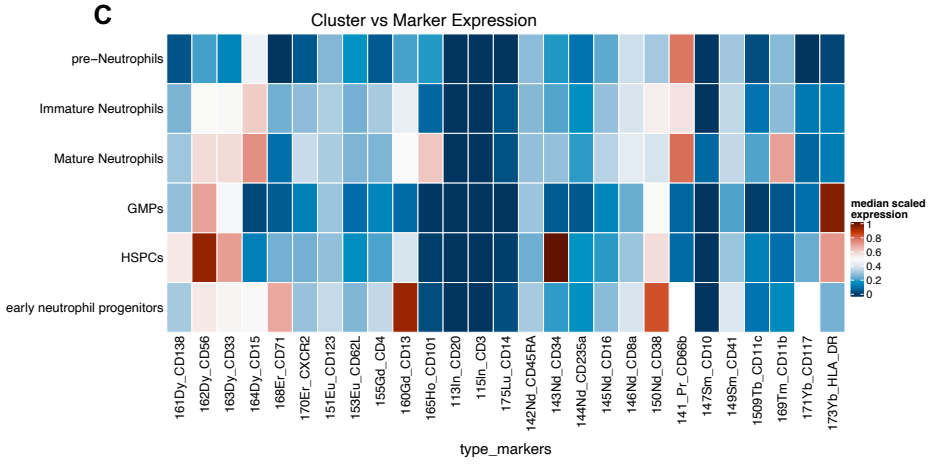

Supplemental Figure 5

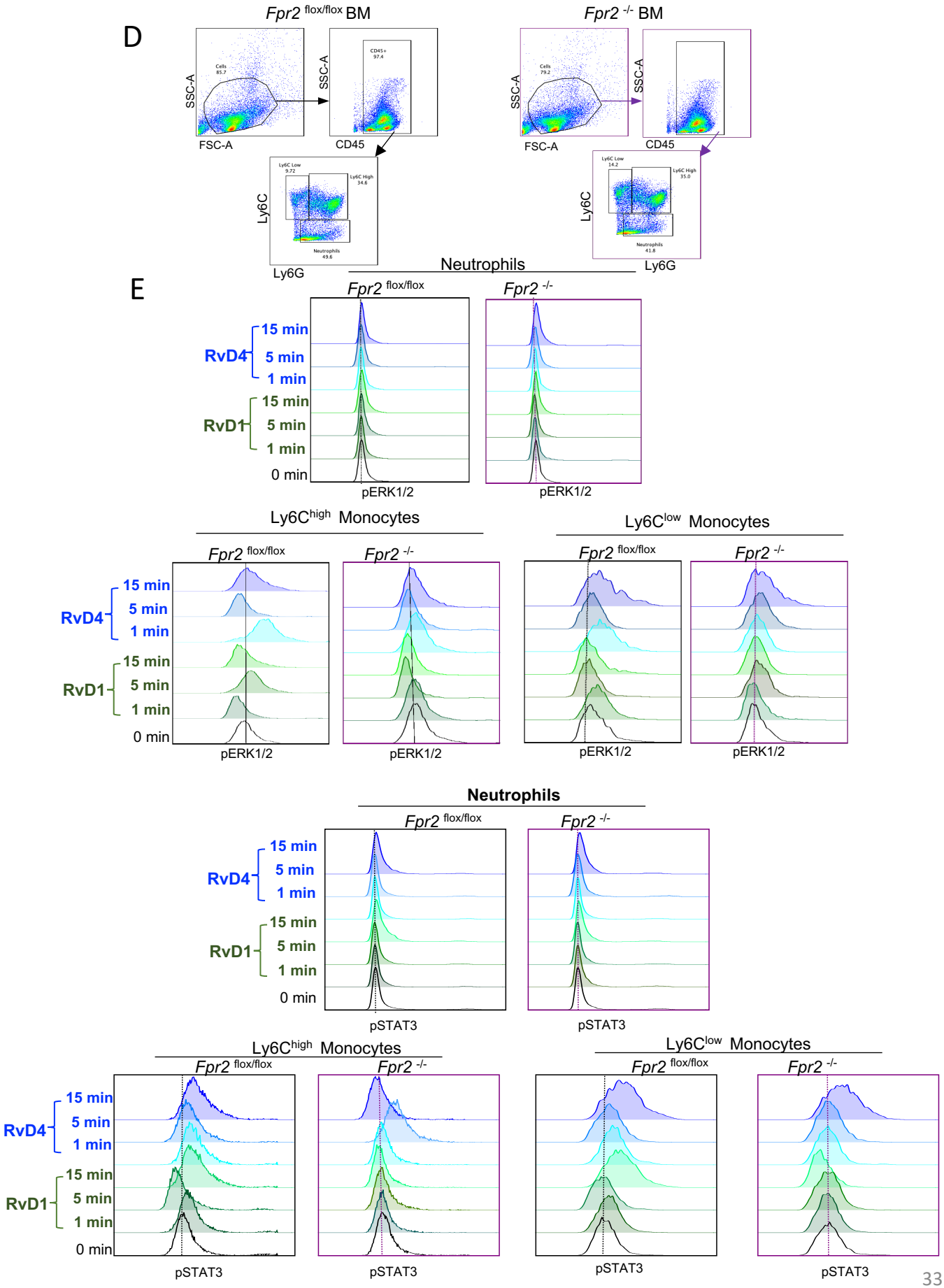

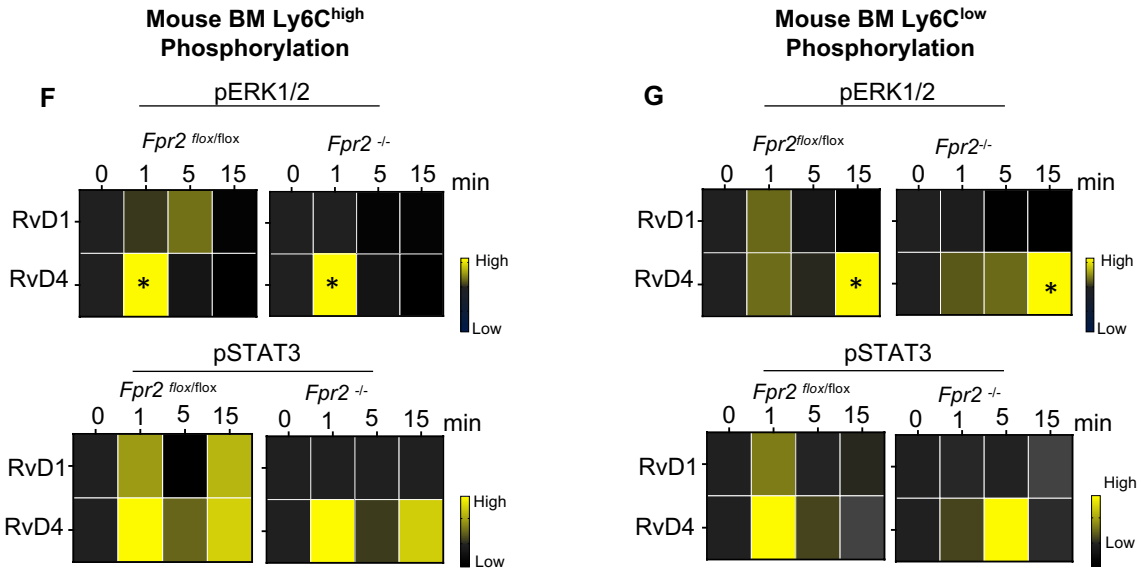

Supplemental Figure 5. RvD4 single-cell phosphorylation signaling in human bone marrow

(A) Gating strategy of human bone marrow for FLOWSOM and UMAP analysis

(B) UMAP Single-cell expression of surface markers in BM populations

(C) Heatmap representing average surface marker expression, highlighting expression sub-set specific markers, such as CD71 on subset early neutrophil progenitor, CD101 on mature neutrophil and CD34 on HSPCs. STAR Methods Resource Table for detail on surface markers. UMAPs and Heatmaps are n=4 human BM samples.

(D) Flow Cytometry Gating Strategy of BM neutrophil ($CD45^{-}Ly6C^{-}Ly6C^{+}$), $Ly6C^{low}$ Monocytes ($CD45^{+}Ly6G^{-}Ly6C^{low}$) and $Ly6C^{high}$ Monocytes ($CD45^{+}Ly6G^{-}Ly6C^{high}$) from ALX/FPR2 $^{flox/flox}$ or ALX/FPR2$^{-/-}$

(E-G) pERK1/2 and STAT3 levels in BM monocytes from *Fpr2* $^{flox/flox}$ or *Fpr2* $^{-/-}$ (ALX deficient mice). (E) Representative histograms of pERK 1/2 and pSTAT3 (F-G), $Ly6C^{high}$ and $Ly6C^{low}$ monocytes heat maps. Phosphorylation levels were calculated as the difference between the geometric mean signal intensity in RvD1 or RvD4 treated BM monocytes (at 0, 1, 5 and 15 min) and the geometric mean signal intensity in vehicle treated BM monocytes at 0 min. Results are expressed as mean ± SEM, n=3 mice from each group. 0 vs. 1, 5 or 15 min *$p<0.05$.

Supplemental Figure 6

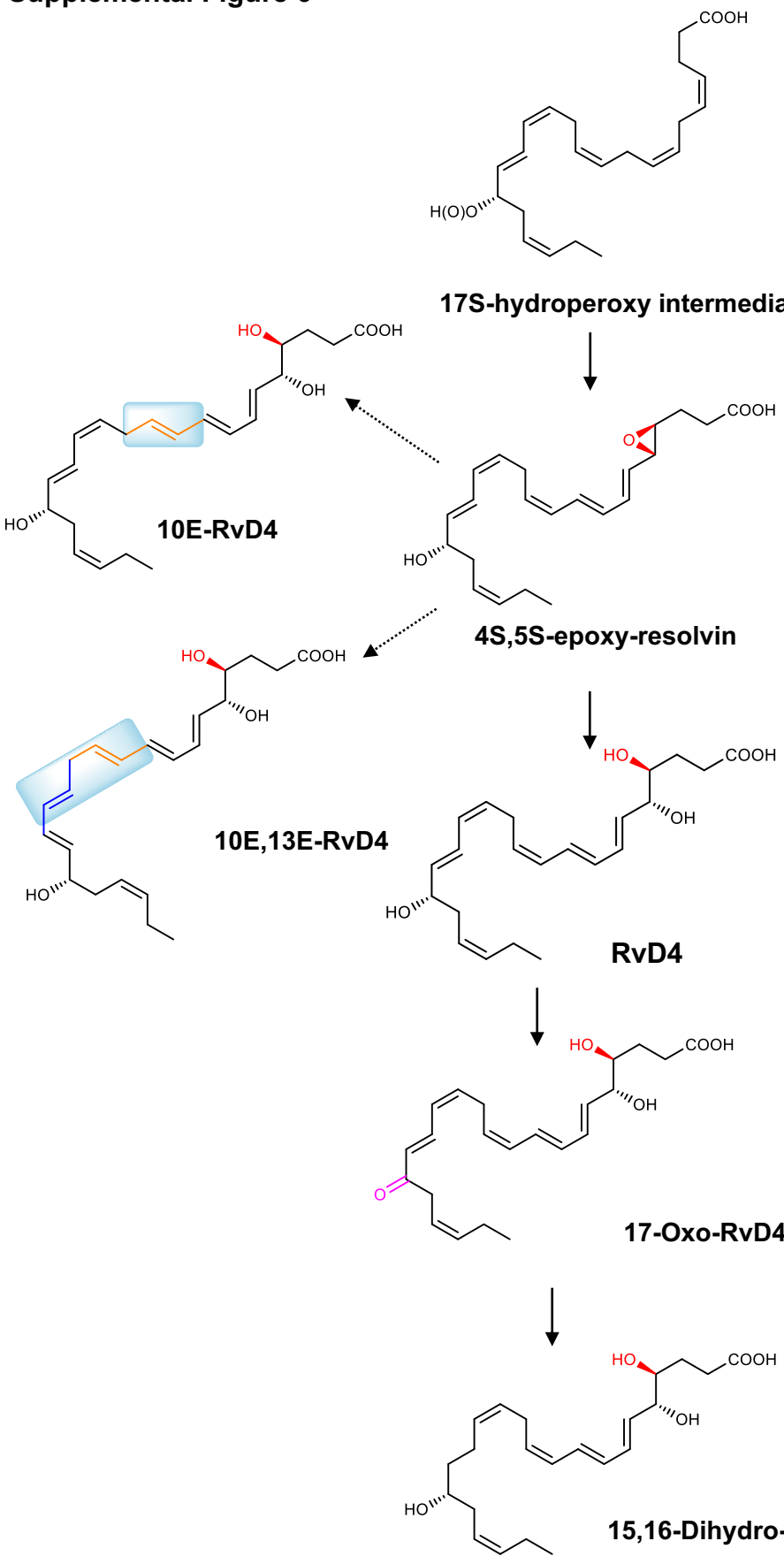

RvD4 Functions

- Limits excessive neutrophil infiltration
- Increases phagocytosis
- Increases macrophage efferocytosis
- Protects from neutrophil mediated second organ injury
- Accelerates the Resolution of Inflammation
- Accelerates the resolution of DVT
- **Regulates excessive neutrophil deployment during infection**

Figure Supplemental 6. Proposed Biosynthesis of Resolvin D4 and its further local metabolic inactivation. RvD4 is formed via a 4,5-epoxide intermediate in a stereo-controlled[1,2]. The structures of 4S, 5S-epoxy-resolvin and RvD4 are depicted in their complete stereochemistry as determined in[1-3]. Non enzymatic hydrolysis of this epoxide formed two products, the 10E-RvD4 and 10E, 13E, RvD4. The two products proved to be biological inactive in leukocytes[2] . RvD4 further is converted to less active metabolites 17-oxo-RvD4 and the 15,16-Dihydro-RvD4 by human BM cells[2]. The less active 17-oxo-RvD4 and 15,16-Dihydro-RvD4 are shown in their most likely configurations based on the stereospecific enzymatic reactions reported in[2].

References

1. Shay AE, Nshimiyimana R, Samuelsson B, Petasis NA, Haeggstrom JZ, Serhan CN. Human leukocytes selectively convert 4S,5S-epoxy-resolvin to resolvin D3, resolvin D4, and a cys-resolvin isomer. *Proc Natl Acad Sci U S A*. 2021;118(51).

2. Winkler JW, Libreros S, De La Rosa X, Sansbury BE, Norris PC, Chiang N, Fichtner D, Keyes GS, Wourms N, Spite M, Serhan CN. Structural insights into Resolvin D4 actions and further metabolites via a new total organic synthesis and validation. *J Leukoc Biol*. 2018.

3.Nshimiyimana R, Lam TF, Aggarwal S, Serhan CN, Petasis NA. First stereoselective total synthesis of 4(S),5(S)-oxido-17(S)-hydroxy-6(E),8(E),10(Z),13(Z),15(E),19(Z)-docosahexaenoic acid, the biosynthetic precursor of resolvins D3 and D4. *RSC Adv*. 2022;12(19):11613-11618.

Table S1. Characteristics of bone marrow donors

BM-Donor #	Gender	Age	BMI	Race	Preparation	Analysis	Cell number per ml	Cell Viability
1	Male	34	26.6	White	Aspirate	CyTOF	$14x10^6$	97%
2	Male	42	33.7	Other	Aspirate	CyTOF	$14x10^6$	98%
3	Male	27	32.1	White	Aspirate	CyTOF	$8X10^6$	97%
4	Male	31	32.6	Black	Aspirate	CyTOF	$14x10^6$	98%

*This table contains demographic information about bone marrow donors. All donors were negative for HIV, HBV, and HCV. Cell viability was determined by flow cytometry using Aqua dead stain.

Table S2. Hematopoietic Cell Populations and Cell Surface Markers*
Identification of immune cell populations in mouse BM, whole blood, and exudate during self-resolving peritonitis infections**

Population	*Abbreviations*	*Surface Expression*
Multipotent Progenitor-1	MPP1	lineage$^-$CD117$^+$SCA1$^+$CD34$^+$CD48$^-$CD150$^+$CD135$^+$ (2)
Multipotent Progenitor-2	MPP2	lineage$^-$CD117$^+$SCA1$^+$CD34$^+$CD48$^+$CD150$^+$CD135$^+$ (2)
Multipotent Progenitor-3 (Myeloid Bias)	MPP3	lineage$^-$CD117$^+$SCA1$^+$CD34$^+$CD48$^+$CD150$^-$CD135$^-$ (2)
Multipotent Progenitor-4 (Lymphoid Bias)	MPP4	lineage$^-$CD117$^+$SCA1$^+$CD34$^+$CD48$^+$CD150$^-$CD135$^+$ (2)
lineage$^-$Sca1$^+$cKit$^+$	LSK	lineage$^-$CD117$^+$SCA1$^+$ (1)
Common Myeloid Progenitor	CMP	lineage$^-$CD117$^+$SCA1$^-$CD16/32$^-$CD34$^+$CD41$^-$ (3)
Granulocyte Myeloid Progenitor	GMP	lineage$^-$CD117$^+$SCA1$^-$CD16/32$^+$CD34^{high}CD41$^-$ (3)
Common Lymphoid Progenitor	CLP	lineage$^-$CD117^{intermediate}CD127$^+$CD135$^+$ SCA1^{low} (4)
Pre-neutrophil	PN	ckit$^+$SiglecF$^-$CXCR4$^+$Ly6G$^-$CXCR2$^-$ (5)
Immature neutrophil	IN	ckit$^-$SiglecF$^-$CXCR4$^+$Ly6G$^+$ CD11b$^+$ (5)
Mature neutrophil	MN	ckit$^-$SiglecF$^-$CXCR4$^-$Ly6G$^+$CXCR2^{high}CD11b$^+$ (5)
Inflammatory Monocytes	IM	Ly6C^{high} CD11b$^+$ CCR2$^+$CX3CR1$^-$CD115$^+$ (5)
Reparative Monocytes	RM	Ly6C^{low} CD11b$^+$ CCR2$^-$CX3CR1$^+$CD115$^+$ (5)
Macrophages	MO	F4/80$^+$CD11b$^+$B220$^-$CD4$^-$CD3$^-$SiglecF$^-$
Eosinophils		CD11b$^+$SiglecF $^+$CD4$^-$CD8$^-$Ly6G$^-$Ly6C$^-$
Basophils		CD11b^{low} SiglecF$^+$ CD4$^-$CD8$^-$Ly6G$^-$Ly6C$^-$CD335$^-$
Myeloid dendritic cells	mDC	CD11b+CD11c$^+$Ly6G$^-$
Plasmacytoid dendritic cells	pDC	CD11b$^-$B220$^+$Ly6C$^+$ SiglecF$^-$
Natural Killer cells	NK	CD335$^+$CD11b$^-$CD3$^-$CD4$^-$
CD4 Effector T cells	CD4-Eff	CD3$^+$CD4$^+$CD44$^+$CD127-
CD4 Memory T cells	CD4-M	CD3$^+$CD4$^+$CD44$^-$ CD127$^+$
CD3 Effector T cells	CD3-Eff	CD3$^+$CD4-CD44$^+$
CD3 Memory T cells	CD3-M	CD3$^+$CD4$^-$CD44$^-$ CD127$^+$
B cells		B220$^+$CD19$^+$CD3$^-$CD11b$^-$Ly6G$^-$B220$^+$CD19$^+$
Platelets		CD41$^+$lineage$^-$Terr119$^+$
Red Blood Cells	RBCs	Terr119$^+$lineage$^-$CD41$^-$

**This table denotes surface markers used for the identification of mouse hematopoietic immune cell populations.

*References

1. Ikuta K, Weissman IL. Evidence that hematopoietic stem cells express mouse c-kit but do not depend on steel factor for their generation. Proc Natl Acad Sci U S A. 1992 Feb 15;89(4):1502-6. doi: 10.1073/pnas.89.4.1502. PMID: 1371359; PMCID: PMC48479

2. Pietras EM, Reynaud D, Kang YA, Carlin D, Calero-Nieto FJ, Leavitt AD, Stuart JM, Göttgens B, Passegué E. Functionally Distinct Subsets of Lineage-Biased Multipotent Progenitors Control Blood Production in Normal and Regenerative Conditions. Cell Stem Cell. 2015 Jul 2;17(1):35-46. doi: 10.1016/j.stem.2015.05.003. Epub 2015 Jun 18. PMID: 26095048; PMCID: PMC4542150

3. Akashi K, Traver D, Miyamoto T, Weissman IL. A clonogenic common myeloid progenitor that gives rise to all myeloid lineages. Nature. 2000 Mar 9;404(6774):193-7. doi: 10.1038/35004599. PMID: 10724173.

4. Adolfsson J, Månsson R, Buza-Vidas N, Hultquist A, Liuba K, Jensen CT, Bryder D, Yang L, Borge OJ, Thoren LA, Anderson K, Sitnicka E, Sasaki Y, Sigvardsson M, Jacobsen SE. Identification of Flt3+ lympho-myeloid stem cells lacking erythro-megakaryocytic potential a revised road map for adult blood lineage commitment. Cell. 2005 Apr 22;121(2):295-306. doi: 10.1016/j.cell.2005.02.013. PMID: 15851035.

5. Ng LG, Ostuni R, Hidalgo A. Heterogeneity of neutrophils. Nat Rev Immunol. 2019 Apr;19(4):255-265. doi: 10.1038/s41577-019-0141-8. PMID: 30816340.

Table S3. Human Hematopoietic Cell Populations and Cell Surface Markers*

Surface markers for identification of populations in human bone marrow**

Population	*Abbreviation*	*Surface Expression*
Hematopoietic Stem and Progenitors cells	HSPCs	lineage^{-}CD34^{+}HLDR^{+}CD45RA^{-} (1)
Granulocyte Myeloid Progenitor	GMP	lineage^{-}CD34^{-}CD16-CD38^{+}CD117^{+}HLDR^{+} (1-2)
Early Neutrophil Progenitor	eNePs	Lineage^{-}CD71^{+}CD117^{+}CD38^{+}CD15^{-}CD34^{-} (3)
Pre-neutrophil	PN	Lineage^{-}CD66b^{+}CD15^{+}CD33^{mid}CD101^{-}CD16^{-}CD11b^{-} HLA-DR^{-} (2)
Immature neutrophil	IN	Lineage^{-}CD66b^{+}CD15^{+}CD33^{mid}CD101^{mid}CD16^{mid}CD11b+ HLA-DR^{-} (2)
Mature neutrophil	MN	Lineage^{-}CD66b^{+}CD15^{+}CD33^{+}CD101^{+}CD16^{+}CD11b^{+} HLA-DR^{-} (2)

**This table denotes surface markers used for the identification of human bone marrow granulocytes.

*References

1. Kondo M, Wagers AJ, Manz MG, Prohaska SS, Scherer DC, Beilhack GF, Shizuru JA, Weissman IL. Biology of hematopoietic stem cells and progenitors: implications for clinical application. Annu Rev Immunol. 2003;21:759-806. doi: 10.1146/annurev.immunol.21.120601.141007. Epub 2002 Dec 17. PMID: 12615892.

2. Ng LG, Ostuni R, Hidalgo A. Heterogeneity of neutrophils. Nat Rev Immunol. 2019 Apr;19(4):255-265. doi: 10.1038/s41577-019-0141-8. PMID: 30816340.

3. Dinh HQ, Eggert T, Meyer MA, Zhu YP, Olingy CE, Llewellyn R, Wu R, Hedrick CC. Coexpression of CD71 and CD117 Identifies an Early Unipotent Neutrophil Progenitor Population in Human Bone Marrow. Immunity. 2020 Aug 18;53(2):319-334.e6. doi: 10.1016/j.immuni.2020.07.017. PMID: 32814027; PMCID: PMC7942809

Table S4. List of mouse antibodies used for mass cytometry*

Antibody	*clone*	*Metal Conjugate*	Source
CD44	IM7	113In	BWH
CD4	RM4-5	115In	BWH
CD45	30-F11	141 Pr	BWH
CD115	AFS98	142 ND	BWH
TER119	TER-119	143 ND	BWH
CXCR4	L276F12	144 ND	BWH
CXC3CR1	SA011F11	146 ND	BWH
CD16/32	93	147Sm	BWH
CD19	6D5	149 SM	BWH
CD127	A7R34	148 ND	BWH
Ly6C	HK1.4	150 ND	Fluidigm
B220/CD45R	RA-3	151 Eu	BWH
CD3	145-2C11	152Sm	BWH
CD335/ NPK46	29A1.4	153 EU	BWH
CD48	HM-48-1	154 SM	BWH
Ly6G	1A8	158 GD	BWH
CD41	MWReg30	159 TB	BWH
CD62L	MEL-14	161 DY	BWH
CD135	A2F10	162 DY	BWH
Ly-6A/E (Sca-1)	D7	164 DY	Fluidigm
CD34	MEC14.7	166 ER	BWH
CD117/ckit	2B8	168 ER	BWH
CXCR2	242216	165HO	BWH
CD11b	M1/70	169TM	BWH
CD170/Siglec F	F-E50	170 ER	BWH
CD150/Slam	TC15-12F12.2	171 YB	BWH
CCR2	SA203G11	174 YB	BWH
F4/80	BM8	175 LU	BWH
CD11c	209BI	209 BI	Fluidigm

*This table contains information about specific anti-mouse antibodies, clones and metal-conjugated used for single mass cytometry (CyTOF) analysis. Some antibodies were obtained from the Longwood Medical Area (LMA) CyTOF antibody resource core at Brigham and Women's Hospital (BWH).

Table S5. List of human antibodies used for mass cytometry#

Antibody	clone	Metal Conjugate	Source
CD45	HI30	89Y	Fluidigm
CD20	*2H7*	*113In*	*BWH*
CD3	*UCHT1*	*115In*	*BWH*
CD66b	GF10F5	141Pr	BWH
CD45RA	HI100	142Nd	BWH
CD34	*581*	143 Nd	BWH
CD235a	HIT2	144 Nd	BWH
CD16	3G8	145 Nd	Fluidigm
CD8a	RPA T8	146 Nd	Fluidigm
CD10	HI10A	*147Sm*	*BWH*
p-STAT4	38	Nd 148	Fluidigm
CD41	HIP8	149 Sm	BWH
CD38	HIT2	*150Sm*	*BWH*
CD123	6H6	*151Eu*	Fluidigm
pAKT (S473)	D9E	*152Sm*	Fluidigm
CD62L	DREG-56	*153Eu*	*BWH*
CD4	RPAT4	155Gd	BWH
p-p38 (T180/Y182)	D3F9	156Gd	Fluidigm
pStat3 (Y705)	4	158Gd	Fluidigm
CD11c	*Bu15*	*159 tb*	*BWH*
CD13	WM15	160Gd	Fluidigm
CD138	MI15	Dy 161	BWH
CD56	HCD56	Dy 162	BWH
CD33	WM53	Dy 163	Fluidigm
CD15	W6D3	164Dy	Fluidigm
CD101	BB27	*165Ho*	Fluidigm
pNF-Kb p65 (S529)	K10-895.12.50	Er 166	Fluidigm
pErk (T202/Y204)	D13.14.4E	Er 167	Fluidigm
CD71	OKT-9	168Er	Fluidigm
CD11b	M1/70	169Tm	BWH
CD182	5E8/CXCR2	170Er	BWH
CD117	104D2	*171Yb*	*BWH*
pS6 (S235/S236)	N7-548	172Yb	Fluidigm
HLA-DR	L243	173Yb	Fluidigm
CD14	M5E2	175Lu	Fluidigm
pCREB (S133)	87G3	176Yb	Fluidigm

#This table contains information about specific anti-human antibodies, clones and metal-conjugated used for single mass cytometry (CyTOF) analysis. Some antibodies were obtained from the LMA CyTOF antibody resource core at Brigham and Women's Hospital (BWH).

Table S6. Liquid chromatography multiple reaction monitoring (LC-MRM) systems on SCIEX QTRAP 5500 and 6500+ instruments*

	Shimadzu LC-20AD		**SCIEX ExionLC**	
Column	Poroshell 120 EC-18 (100 mm x 4.6 mm x 2.7 µm) Agilent Technologies		Kinetex Polar C18 (100 mm X 4.6 mm X 2.6 µm) Phenomenex	
Solvent A	Water (0.01% acetic acid)		Water (0.1% formic acid)	
Solvent B	Methanol (0.01% acetic acid)		Methanol (0.1% formic acid)	
Flow Rate	0.5 mL/ min		0.5 mL/ min	
Gradient	Time (min)	Solvent B (%)	Time (min)	Solvent B (%)
	0.0	Start	0.0	Start
	0.2	50	0.1	45
	2.0	50	2.0	45
	11.0	80	16.5	80
	14.5	80	16.6	98
	14.6	98	18.5	98
	20.0	98	18.6	10
	20.1	20	20.9	Stop
	23.0	Stop	-	-
	AB SCIEX QTRAP 5500		**SCIEX QTRAP 6500+ (Low Mass Mode)**	
	MRM and EPI Mode		MRM and EPI Mode	
Curtain Gas	25.0		30.0	
Collision Gas	Medium		12.0	
Ion Spray Voltage (V)	-4000		-4200.0	
Temperature (°C)	500.0		520.0	
Ion Source Gas 1 (psi)	60.0		85.0	
Ion Source Gas 2 (psi)	60.0		50.0	

*Detailed information on columns, solvent systems, flow rates (mL/ min), mobile phase gradients, and multiple reaction monitoring (MRM) and enhanced product ion (EPI) settings for both SCIEX QTRAP 5500 and SCIEX 6500+ Triple Quadrupole mass spectrometers in negative polarity: curtain gas, collision gas, ion spray voltage (V), temperature (°C), ion source gas 1 (psi), and ion source gas 2 (psi).

Table S7. Tandem mass spectrometry ion pairs, deuterium-labeled internal standards (IS) and detection parameters used for select lipid mediators analyzed on SCIEX triple quadrupole QTRAP 5500 and 6500+ mass spectrometers[†]

Targeted Analyte	Q1 > Q3	IS used	CE (V)	CXP (V)
AB SCIEX QTRAP 5500				
17-HDHA	343 > 245	d_8-15*S*-HETE	-17	-14
RvD1	375 > 215	d_5-RvD2	-26	-13
RvD4	375 > 101	d_5-RvD3	-22	-16
RvD5	359 > 199	d_4-LTB_4	-21	-13
7-HDHA	343 > 141	d_8-5*S*-HETE	-18	-15
4-HDHA	343 > 101	d_8-5*S*-HETE	-17	-15
18-HEPE	317 > 259	d_8-15*S*-HETE	-16	-23
RvE1	349 > 195	d_5-LXA_4	-22	-12
15-HEPE	317 > 219	d_8-15*S*-HETE	-18	-12
12-HEPE	317 > 179	d_8-12*S*-HETE	-19	-12
5-HEPE	317 > 115	d_8-5*S*-HETE	-18	-12
SCIEX QTRAP 6500+				
RvD1	375 > 215	d_5-RvD2	-21	-12
RvD4	375 > 101	d_5-RvD3	-22	-12

[†]Parent-daughter mass transitions (Q1 > Q3, *m*/*z*), deuterated lipid mediator internal standards, collision energies (CE, V), and collision cell exit potentials (CXP, V), for SCIEX QTRAP 5500 and 6500+ LC-MS/MS systems. Declustering potentials (DP, V) and entrance potentials (EP, V) were set at -80 and -10, respectively, for the QTRAP 5500, as well as at -40 and -10 for QTRAP 6500+. All listed mediators were acquired in negative ionization mode on both instruments.